



THE INSTITUTE OF PAPER CHEMISTRY, APPLETON, WISCONSIN

STATUS REPORTS

To The

Engineering Project Advisory Committee

March 23-24, 1989
The Institute of Paper Chemistry
Continuing Education Center
Appleton, Wisconsin

NOTICE & DISCLAIMER

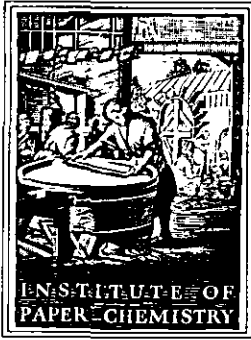
The Institute of Paper Chemistry (IPC) has provided a high standard of professional service and has exerted its best efforts within the time and funds available for this project. The information and conclusions are advisory and are intended only for the internal use by any company who may receive this report. Each company must decide for itself the best approach to solving any problems it may have and how, or whether, this reported information should be considered in its approach.

IPC does not recommend particular products, procedures, materials, or services. These are included only in the interest of completeness within a laboratory context and budgetary constraint. Actual products, procedures, materials, and services used may differ and are peculiar to the operations of each company.

In no event shall IPC or its employees and agents have any obligation or liability for damages, including, but not limited to, consequential damages, arising out of or in connection with any company's use of, or inability to use, the reported information. IPC provides no warranty or guaranty of results.

This information represents a review of on-going research for use by the Project Advisory Committees. The information is not intended to be a definitive progress report on any of the projects and should not be cited or referenced in any paper or correspondence external to your company.

Your advice and suggestions on any of the projects will be most welcome.



THE INSTITUTE OF PAPER CHEMISTRY

Post Office Box 1039
Appleton, Wisconsin 54912
Phone: 414/734-9251
FAX: 414/738-3448
Telex: 469289

March 6, 1989

TO: Members of the Engineering Project Advisory Committee

Enclosed is advance reading material for the March 23-24 meeting of the Engineering Project Advisory Committee. Included are status reports for active projects, an agenda, and a current committee membership list.

Rooms have been reserved in the Continuing Education Center, and meals will be provided as stated on the agenda. If you haven't already indicated your attendance, please do so at your earliest convenience by returning your registration form or calling Jennifer Schuh at 414/738-3320. Also enclosed is the Security Card with the number to gain entrance into the Continuing Education Center.

For all Project Advisory Committee meetings, the Institute invites its member companies to send one or more representatives to attend the review sessions (first day) of any or all of the meetings. These invitations were mailed in February. PAC members from member companies are also welcome to attend the other meetings, and may stay in the CEC and attend meetings and meals of their choice, at no cost. If you wish to attend any of the other meetings, but haven't registered, please call Jennifer Schuh to do so. A meeting schedule is enclosed for your information.

We look forward to meeting with you on March 23-24.

Sincerely,

Ronald A. Yeske
Vice President
Research and Academic Affairs

RAY/lms
Enclosures

THE INSTITUTE OF PAPER CHEMISTRY

Project Advisory Committee Spring Meetings
Member Dues-Funded Research Reviews

March 21, 22, 23, 28, and 29

1989

Continuing Education Center
Appleton, Wisconsin
(414) 734-9251

<u>Committee</u>	<u>Review Schedule</u>	<u>Research Area*</u>
Pulping Processes	Tuesday, March 21 8:30 a.m. - 5:30 p.m. Dinner at 6:00 p.m.	Kraft Chemical Recovery Furnace Processes Chemical Pulp Alkali Pulping Oxygen Bleaching Chlorinated Organics Analytical Techniques Microstructure of Wood Fibers High Lignin Pulps Photochemistry
Paper Properties	Wednesday, March 22 8:30 a.m. - 5:30 p.m. Dinner at 6:00 p.m.	Board Properties and Performance Process, Properties, Product Relationships Internal Strength Enhancement Strength Improvement and Failure Mechanisms On-line Measurement of Paper Mechanical Properties Fundamentals of Paper Surface Wettability
Engineering	Thursday, March 23 10:00 a.m. - 5:30 p.m. Dinner at 6:00 p.m.	Corrosion Recovery Boiler Fireside Corrosion Kraft Liquor Corrosivity Suction Roll Failures Papermaking Displacement Pressing Wet Pressing Impulse Drying

**Not in order of agenda*

Committee

Review Schedule

Research Area*

Systems Analysis

Tuesday, March 28
1:00 p.m. - 5:30 p.m.

Dinner at 6:00 p.m.

MAPPS Marketing Strategy
MAPPS Simulator Development
Continuing System Development
Performance Attribute Modeling
Optimization with MAPPS
MAPPS Applications and
Field Experience

Forest Biology

Wednesday, March 29
1:00 p.m. - 5:00 p.m.

Dinner at 6:00 p.m.

Softwood Somatic Embryogenesis
Initiation
Development/Maturation
Conversion
Biochemistry of Embryo Development
Hardwood Cloning

TABLE OF CONTENTS

	<u>Page</u>
TABLE OF CONTENTS	i
AGENDA	ii
COMMITTEE LIST	iv
STATUS REPORTS	
Project 3628: Recovery Boiler Fireside Corrosion	1
Project 3556: Fundamentals of Kraft Liquor Corrosivity	10
Project 3309: Fundamentals of Corrosion Control in Paper Mills	17
Project 3470: Fundamentals of Drying	22
Project 3480: Fundamentals of Wet Pressing	47

AGENDA

ENGINEERING PROJECT ADVISORY COMMITTEE MEETING

March 23-24, 1989

Continuing Education Center (CEC)
The Institute of Paper Chemistry
Appleton, Wisconsin

Thursday, March 23, 1989

10:00am	-- INTRODUCTION	Yeske/Rounsley
10:15	-- ATLANTA RELOCATION UPDATE	Yeske
	-- CORROSION AND MATERIALS ENGINEERING GROUP	
10:45	- Recovery Boiler Fireside Corrosion	Ahlers
11:15	- Fundamentals of Kraft Liquor Corrosivity	Ahlers
11:45	LUNCH	
1:00pm	- Fundamentals of Corrosion Control in Paper Mills	Yeske
	-- PAPERMAKING PROCESSES GROUP	
1:30	- Fundamentals of Drying	Orloff
2:30	- Fundamentals of Wet Pressing	Lindsay
3:15	-- BREAK	
3:30	- Roll Press Developments	<i>Cyrus</i> Aidun
3:45	- Fundamentals of Coatings	<i>Cyrus</i> Aidun
4:00	- Corrosion Control in Electrostatic Precipitators	Thompson
5:30	-- COCKTAILS	
6:00	-- DINNER - CEC DINING ROOM	

Friday, March 24, 1989

7:15am -- BREAKFAST - CEC DINING ROOM

COMMITTEE ACTIVITIES

8:00am -- Project Reviews

Committee and Staff

9:30 BREAK

9:45 -- Continued Discussion

10:30 -- Report Preparation

Committee

11:00 -- Adjourn

 -- LUNCH - CEC DINING ROOM

ENGINEERING
Project Advisory Committee

Dr. Robert Rounsley (Chairman) - 6/89*
Research Fellow
Mead Corporation
8th & Hickory Streets
Chillicothe, OH 45601
(614) 772-3581

Mr. Sven S. Arenander - 6/90
Group Leader
Union Camp Corporation
P.O. Box 3301
Princeton, NJ 08543-3301
(609) 896-1200

Mr. Percy E. Brooks - 6/90
Manager, Pulp & Paper Engineering
Georgia-Pacific Corporation
133 Peachtree Street, N.E.
P.O. Box 105605
Atlanta, GA 30348-5605
(404) 521-4618

Mr. David J. Lacz - 6/91
Senior Development Engineer
Eastman Kodak Company
Building 319
Kodak Park
Rochester, NY 14650
(716) 458-1000

Dr. Henry Luming - 6/91 - *Oriental*
Project Manager
Stone Container Corporation
Engineering Technology
8170 South Madison Street
Burr Ridge, IL 60521
(312) 655-6945

Mr. Richard J. Posey - 6/91
Technical Services Superintendent
Great Southern Paper Company
P.O. Box 44
Cedar Springs, GA 31732
(912) 372-5541

Mr. Bharat B. Shah - 6/91
Manager of Technical Services
Wisconsin Tissue Mills Inc.
P.O. Box 489
Menasha, WI 54952
(414) 725-7031

Sandy
Dr. W.B.A. Sharp - 6/90
Group Leader
Westvaco Corporation
Laurel Research Center
11101 Johns Hopkins Road
Laurel, MD 20707
(301) 792-9100

Dr. John Smuk - 6/89
Manager of Process Engineering
Research and Development Center
Potlatch Corporation
P.O. Box 510
Cloquet, MN 55720
(218) 879-2393

Mr. Benjamin Thorp - 6/89
Senior Vice President
Research and Engineering
James River Corporation
P.O. Box 2218
Richmond, VA 23217
(804) 644-5411

Dr. Jerry Wallace - 6/89
Mill Manager
Appleton Papers Inc. *Now in Appleton*
East Main Street
Roaring Springs, PA 16673-1480
(814) 224-2131

Dr. Donald A. Wensley - 6/91
Engineering Associate *Long curly hair*
MacMillan Bloedel Inc.
3350 East Broadway
Vancouver, BC V5M 4E6
CANADA
(604) 254-5151

Dr. Yung Duk Woo - 6/89
Senior Engineer
Papermaking R&D Department
Weyerhaeuser Paper Company
Tacoma, WA 98477
(206) 924-6428

2/89

*date of retirement

S T A T U S R E P O R T S
To The
Engineering Project Advisory Committee

March 23-24, 1989
The Institute of Paper Chemistry
Continuing Education Center
Appleton, Wisconsin

THE INSTITUTE OF PAPER CHEMISTRY
Appleton, Wisconsin

Status Report
to the
ENGINEERING PROJECT ADVISORY COMMITTEE

Project 3628
RECOVERY BOILER FIRESIDE CORROSION

March 23-24, 1989

PROJECT SUMMARY FORM

DATE: March 23, 1989

PROJECT NO.: 3628 - RECOVERY BOILER FIRESIDE CORROSION

PROJECT LEADER: Per-Erik Ahlers

IPC GOAL:

Improve safety and increase the operating life of equipment by proper selection of construction materials and by identifying suitable process conditions.

OBJECTIVE:

To understand the causes of corrosion in the kraft recovery boiler, as a basis for devising methods of reducing corrosion damage.

CURRENT FISCAL BUDGET: \$75,000

SUMMARY OF RESULTS SINCE LAST REPORT: (September 1988 - February 1989)

Laboratory studies to accomplish a previously planned testing program have resumed. The test gas mixture does not seem to be aggressive immediately after the components are mixed together at the elevated temperature, but rather after a short time period. Corrosion on carbon steel is accelerated in the presence of simulated smelt powder at 300 and 400°C.

A corrosion probe using air as a temperature control medium has been designed and constructed to be used in field experiments. It provides possibilities to conduct, not only weight loss measurements, but electrical and electrochemical measurements as well.

Assembly of a laboratory apparatus to be used for electrochemical measurements in molten salts under controlled atmosphere has begun.

Efforts have been made to get field experiments started in a CE-boiler furnace using an air cooled corrosion probe.

INTRODUCTION:

Fireside corrosion of recovery boiler components in the lower furnace has been a chronic problem. The primary concern is the possibility of a smelt explosion if water leaks into the boiler due to perforation of corrosion-thinned water tubes or smelt spouts, with possible injury to personnel and loss of production. Higher operating costs include periodic inspection and repairs, plus downtime. Moreover, the cost of insurance has been increasing due to the large number of recovery boiler accidents.

The corrosion mechanism is not known in detail and neither are all of the factors influencing it. Efforts to initiate laboratory and field tests have begun. The objective of field testing is to identify the corrosion conditions prevailing in the lower part of furnace. These conditions will be simulated in laboratory experiments to study different factors in detail under controlled conditions.

Air port corrosion involves the wastage of stainless steel from composite tube air ports to expose the underlying carbon steel. This serious problem has been attributed to NaOH condensation. Alternative mechanisms for this corrosion have also been proposed.

Corrosion resistance of stainless steel relies on the resistance of surface films of chromium oxide, which in many cases gives good protection to the underlying alloy. It is very unlikely that hot gas scaling would destroy

the passive layer in wind box area, since the temperature is too low for that to occur. Consequently, a liquid phase or frozen melt might be the medium that affects a breakdown of the passivity on the back side of composite water wall tubes.

Generally speaking, corrosion in molten salts depends on the oxidizing power (redox potential) and their chemical aggressiveness. In the wind box area, oxidizing conditions prevail. The medium that destroys the passivity under oxidizing conditions is most likely a liquid having strong flexing properties. There are only a few compounds that come under consideration: alkali hydroxides, bisulfates, and polysulfides. Pyrosulfates in combination with chloride are also suggested to be responsible for corrosion on the back side of composite tubes.

The acidity of melts is controlled by the gas atmosphere. Water vapor content in the gas phase, for instance, causes molten hydroxide to turn acidic. It is known that the acidity or basicity affect the corrosion properties substantially. The corrosion behavior may be predicted based on results from electrochemical measurements.

PROGRESS:

Tube Furnace Laboratory Studies

The apparatus used for laboratory experiments is described in the status report for the PAC spring 1988 meeting. It consists of a horizontal tube furnace (ID 2 inches), with one end of the tube connected to gas supply piping and the other to an outlet system for waste gas collection. Previously, three long-term runs (one month) had taken place under a nitrogen gas atmosphere at 300, 400, and 500°C, with carbon and stainless steel coupons placed in ceramic ships covered with synthetic smelt powder. The measured average corrosion rate

was low, in the range of 0.4 - 10 mpy, and was much the same for both steels tested. The effect of temperature was small, indicative of diffusion control through the corrosion layer. It should be noted that the smelt must be responsible for the corrosion obtained in the experiments with an inert gas atmosphere, indicating some degree of chemical instability of the constituents in the salt mixture.

Short term corrosion experiments (5 hours) with an aggressive gas containing H_2S and O_2 have been carried out to identify a more appropriate test procedure. Two ceramic boats with one carbon steel coupon in each were used in each test. It soon became evident that the original conditions of gas flow to the furnace were too slow. Changes in the gas supply system had to be made to replenish the aggressive gases close to the corrosion coupons in the furnace.

Table 1 gives the test conditions with corrosion results. The weight loss and weight gain were measured. The ratio of weight loss (following corrosion product removal) to weight gain gives information regarding the corrosion process; i.e., if they have been oxidizing or sulfidizing. The weight ratio for magnetite (Fe_3O_4) is 2.6, and that for FeS is 1.8. These two corrosion products are the most likely to be formed. The ratios obtained were usually close to that for magnetite indicating an oxidizing environment. This was considered appropriate because the strongly reducing constituents, hydrogen or carbon monoxide, were not present.

Grit blasting is used for removing corrosion products from corrosion coupons. The loss of uncorroded metal was experienced if sandblasting procedure was carried out at too high a pressure or for too long a time. The wastage of uncorroded metal was tested in order to find the right procedure, and an average figure of 1.2 mg metal loss was found to be the best result. This amount was deemed to be acceptably small.

Table 1. Results from tube furnace experiments in pure gas atmosphere. The gas composition before entering the furnace expressed in vol-%: 1% H₂S, 1% O₂, 2% H₂O, 10% H₂O, and balance N₂. Carbon steel coupons of grade A210 with a total surface area of 25 cm² were used.

Temp °C	Gas Flow L/hr	Weight Gain mg	Weight Loss mg	Corrosion Rate mpy
300	1.5	4.2	41.7*	146*
	1.5	3.1	62.2*	218*
300	9	5.6	17.0	60
	9	7.8	16.2	57
400	1.5	11.4	24.7	87
	1.5	11.5	25.1	89
400	9	14.0	28.1	100
	9	11.6	27.8	99

*erroneous due to improper gritblasting

Table 2. Results from corrosion experiments with carbon steel coupons (A210) embedded in simulated smelt powder. Gas composition as in Table 1. The powder composition: 80% Na₂CO₃, 12% Na₂SO₄, and 8% Na₂S.

Temp °C	Gas Flow L/hr	Weight Gain mg	Weight Loss mg	Corrosion Rate mpy	Effective Surface Area %
300	1.5	N.D.	25.6	145	61
	1.5	N.D.	30.3	172	61
300	9	8.0	20.1	114	61
	9	8.3	21.5	122	61
400	1.5	15.1	35.5	199	65
	1.5	15.0	35.8	201	65
400	9	17.0	48.9	275	65
	9	15.1	44.4	249	65

The effect of gas velocity was investigated in a range from 1.5 to 9 L/hr. It appeared that the flow rate had only a marginal effect at 300 and 400°C, and therefore a rate of 3 L/hr was chosen to be used in the following experiments. From the result with two coupons at different locations in the

furnace, it was hypothesized that the gas mixture in the furnace became more corrosive after a short time period perhaps because of reactions in the gas mixtures.

Comparison of the corrosion results in Table 1 and 2 shows that the presence of the salt increased the corrosion. This is an unexpected result because the powder around the coupons must restrict the gas diffusivity. A layer of powder approximately 2 mm thick was covering the corrosion coupons in these tests. The bottom surfaces of the test coupons resting on the powder bed were hardly attacked in these experiments. The corrosion rate was calculated by using an effective area, where only a fraction of the attacked bottom surface was taken into account. The reason for the contribution of powder to corrosion is not known at present.

Wind Box Corrosion Probe

A corrosion probe for field testing has been designed and constructed. The probe, as shown in Figure 1 below, uses hot and cool air to control the temperature of a circular and changeable corrosion coupon. Deposits will be collected on the coupon at different surface temperatures. The probe provides facilities for electrical conductivity and electrochemical measurements.

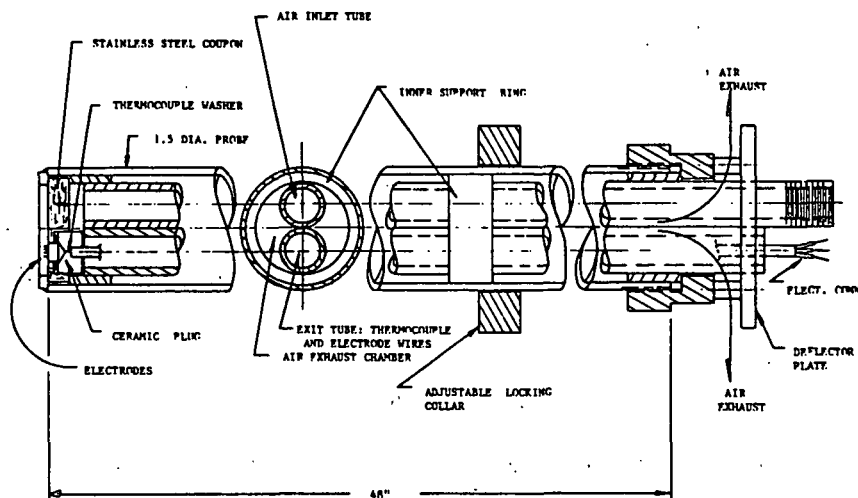


Figure 1. Construction of corrosion probe

Electrochemical Studies in Molten Salts

Assembly of equipment for electrochemical studies has begun. This equipment will be used to determine polarization curves for stainless steel in hydroxide melts of varying acidity. A small vertical tube furnace will be used for these tests; a stainless steel retort has been constructed for insertion into the furnace. A Zirconia reference electrode will be used. This electrode can also be used for the production of oxygen ions to control the water content in the melt.

Fire Box Corrosion Probe

An air cooled corrosion probe is under design. One purpose of the field experiments planned for a CE boiler is the identification of corrosive environments and their relation to the average corrosion rate obtained with the temperature controlled coupons. Another possible purpose is instantaneous corrosion rate measurements using electrochemical methods.

PLANS FOR NEXT PERIOD:

The program previously planned will be followed to study the effect of NaOH, NaCl, Na₂S₂O₇, KCl, Na₂S₂O₃, S₈, and NaSO₃ additions to the simulated smelt powder on carbon steel and stainless steel specimens.

Polarization curve determination will be performed in low temperature molten salts to determine what conditions stainless steel are required to destroy passivity and where stainless steel is most susceptible to corrosion.

Corrosion probe field experiments will be started in a B & W boiler in order to perform corrosion rate measurements and to collect deposits at controlled temperatures. Access to the boiler for the probe has been established. Plans to build an additional access port are being considered. The probe has been constructed and field tested.

Prior to the next meeting, the hot side corrosion probe will be built and test results are available.

SIGNIFICANCE TO THE INDUSTRY:

An improved knowledge of corrosion mechanisms in recovery boilers will aid in the design and/or remedial measures which will extend the operating life and improve safety.

THE INSTITUTE OF PAPER CHEMISTRY
Appleton, Wisconsin

Status Report
to the
ENGINEERING PROJECT ADVISORY COMMITTEE

Project 3556
FUNDAMENTALS OF KRAFT LIQUOR CORROSIVITY

March 23-24, 1989

PROJECT SUMMARY FORM

DATE: March 23, 1989

PROJECT NO.: 3556 - FUNDAMENTALS OF KRAFT LIQUOR CORROSIVITY

PROJECT LEADER: Staff

IPC GOAL:

Increase the service life of equipment by proper selection of materials and of construction and by identifying suitable process conditions.

OBJECTIVE:

To understand the causes of corrosion and corrosion-assisted cracking of carbon steels exposed to kraft liquor as a basis for developing methods for reducing corrosion damage in kraft liquor streams.

CURRENT FISCAL BUDGET: \$75,000

SUMMARY OF RESULTS SINCE LAST REPORT: (September 1988 - February 1989)

Investigation of the effect of flow rate on corrosion by using rotating cylinder of carbon steel has continued in hot simulated white liquor with potential control at -0.2 V vs. SSSE. The repeatability of results was not improved despite using a lower potential and remedies undertaken to minimize vibrations. In view of the continuing difficulties experienced with the existing apparatus, and the imminent termination of this project, further studies of flow rate effects have been abandoned to redirect personnel to other project areas.

INTRODUCTION:

Corrosion rates in kraft white liquor usually increase with flow rate. Measurements made in mills have shown this effect is especially pronounced in piping. Typical white liquor design velocities are from 1 to 5 ft/s in troughs, from 6 to 7 ft/s in underflow lines from the clarifier, and from 8 to 10 ft/s in

pumped 6 to 8 inch lines. Stainless steel could be used in many of these locations. An improved understanding of the relationship between the corrosion rate and the liquid velocity would assist equipment designers in sizing equipment or choosing materials to minimize the costs of corrosion.

Testing of the effects of velocity using pipe loops is cumbersome and slow, and involves large quantities of liquor. The rotating cylinder electrode (RCE) is an alternative method, which allows systematic and relatively rapid investigation of the effects of flow rate. Smaller quantities of liquor may be used compared to flow loops, providing better control of liquor conditions.

The objective of this work is to develop a RCE technique to be used for studies of velocity effects on corrosion in kraft liquors. This test method could be used to develop data to provide pipe designers so they can relate flow parameters such as flow rate in pipes to corrosion rate.

PROGRESS:

The rotating cylinder electrode assembly used for this experiment has been described in detail in the PAC Status Report for the Spring, 1988 meeting. Prior to the last meeting, potential control was applied by potentiostat to the rotating cylinder electrode in order to improve the reproducibility of results. The potential first applied was chosen to be close to the rest potential obtained from polarization curves (-0.15 V vs. SSSE). No essential improvement in the repeatability took place when using potential control. The reason was deemed to be the high potential, which kept the working electrode in the unstable active part of the polarization curves. It was decided to lower the potential by 50 mV to be -0.2 V vs. SSSE in the subsequent runs.

Table 1 gives the weight loss results and information of test conditions in the latest 9 runs. Two rotation speeds, 1000 and 2000 RPM, were

used. The 1000 RPM corresponding to a periphery velocity of 0.48 m/s (1.57 ft/s) and that for 2000 RPM to 0.96 m/s (3.15 ft/s), respectively. A specific procedure was undertaken before each run to stabilize test conditions. It included the following steps: increasing the temperature (90°C), immersion of electrode into the hot solution, applying a potential of -0.5 V vs. SSSE increasing the electrode potential slowly to -0.2 V, and holding the electrode at these conditions (90°C, -0.2 V stagnant) for two hours. The test was then started by bringing the electrode up to the desired rotation rate. The test duration was 48 hours, with exceptions of the two slightly longer runs over weekends. Previous test data have shown that the length of testing is not very critical.

Table 1. Results from corrosion tests conducted at -0.2 V vs. SSSE with carbon steel cylinder of grade C1018 in white liquor containing 100 g/L NaOH and 30 g/L Na₂S under nitrogen blanket. The surface area was 9 cm².

Run	Speed, RPM	Duration, hours	Current in mA		Corrosion Rate, mpy
			Init.	Final	
1	1000	48	-0.34	- 5.2	36
2	1000	48	-0.20	- 0.95	51
3	1000	96	-0.14	- 3.8	41
4	1000	66	-0.55	- 4.5	37
5	2000	48	-0.40	-50	224
6	2000	48	-5.5	-32	38
7	2000	48	-1.0	-10	16
8	2000	48	-0.85	- 3.5	21
9	1000	48	-0.92	- 9.2	25

shorten the electrode shaft by 1" to 5"

The first four runs were promising, giving corrosion results with relatively little scatter. When the rotation speed was increased in run 5 to 2000 RPM, the corrosion rate increased by a factor of five (224 mpy). At this higher speed, the electrode shaft and the motor assemble vibrated substantially. In order to minimize the vibration, the electrode shaft was shortened by one inch (i.e., 5 inches long). The next three runs were carried out at the same higher speed, but the corrosion rate became almost one order of magnitude lower. In

*3.20
5
16.40* *16.4
60
98 4.0*

the last run, the electrode was rotated at the lower speed of 1000 RPM. The corrosion rate in this test was essentially the same as that obtained in runs 6 to 8 at 2000 RPM.

The current demand for potential control was in all runs cathodic, and increased throughout testing, indicating that the free potential was shifted in the positive direction. If no significant changes in the cathodic conditions (oxidizing species) took place during the test period, this trend indicates that the electrode tended to be less active, perhaps as a result of deposit formation.

DISCUSSION:

After the 9th run, it was decided that the performance of electrode had to be improved before the work could continue. The main reason for the vibrations was the long and relatively thin electrode shaft. The fitting of the electrode shaft to motor shaft did not provide adequate alignment of the electrode. Unbalance can also result from an uneven corrosion path, but that was deemed to have a minor effect.

Different remedies were considered. One alternative was to rebuild the electrode assembly to improve alignment. Another alternative was to purchase a commercial rotator having a well designed electrode shaft fitting. Commercial rotating cylinder electrodes are not available, but electrode shafts are, which can easily be modified to be usable. The cell compartment would have to be modified to accommodate any changes in the rotating electrode configuration.

The main objective of this project is to develop a simple method for testing the effect of liquid velocity on corrosion by using a cylindrical rotating electrode. The experience gained with the rotating electrode in white liquor has taught that the rotating electrode movement path in the test solution

is critical and must be rather smooth. Vibration induces unstable turbulence and obviously tends to spall off corrosion products from the electrode surface in an uncontrollable manner.

It must also be kept in mind that potential control does not work properly in all flow rate regimes. In stagnant liquid or with laminar flow mode, the stagnant liquid layer adhered to metal surface is relatively thick and diffusion control is usually in effect (in white liquor, cathodic control exists). Under such conditions, the corrosion rate will be less dependent on the electrode potential and consequently, potential control will have a limited effect. A transition from laminar to turbulent flow mode occurs smoothly in the low flow rate range (<0.5 m/s) and the velocity effect increases by reducing the stagnant liquid layer and thereby increasing the rate of corrosion. At some point in the turbulent range, the stagnant layer becomes so thin that diffusion does not restrict corrosion rate. The limiting factor will be charge transfer (activation polarization), where the corrosion rate responds fully to electrode potential. With potentiostatic control, the corrosion rate becomes independent of the flow rate. Corrosion can even decrease with increasing flow rate in this flow range if the corrosion rate is high and close to the critical rate where passivation begins to take place. Obviously, the corrosion conditions are labile in this important flow rate regime. Thus, for a flow rate simulation to be successful, well-defined flow conditions are required. When cavitation sets in at a high velocity range, at flow rates over 5-10 m/s, the liquid flow destroys the corrosion layer and can remove particles of the metal. Obviously potential control does not have any effect here. Erosion is very marked if solid particles are present.

FUTURE PLANS:

It seems to be difficult under laboratory conditions to simulate both the hydrodynamic and corrosion condition existing in the process piping. For a more successful trial, a significantly improved electrode rotation system must be used. Furthermore, potential control is not appropriate for use in this connection because it is effective only under certain flow rate range, and will mask the effect of the flow rate.

It would be preferable to conduct such a study in mill site by using a bypass loop with controllable flow rate. However, results obtained in this way might be consistent only for the particular process and conditions where the experiments are done. To gain a more general view of the effect of flow rate in kraft liquors, the study should cover a number of mills.

In view of the termination of Project 3556 in June, we propose to suspend this project. If the problems related to flow rates are still considered of great importance, a new project can be planned based on experience from this project. Alternatively, this final aspect of liquor corrosivity project could be completed through further student projects.

SIGNIFICANCE TO THE INDUSTRY:

In tests of the effect of velocity on corrosion in white liquor, very high corrosion rates have been measured, confirming the importance of flow on corrosion rates. Considerable scatter has been observed, even when the corrosion potential is controlled. This is similarly true in the pipe flow loop. In some areas in the turbulence flow range, corrosion rate is not always inevitable with increasing flow rate, explaining partly why it is so difficult to produce reproducible results.

THE INSTITUTE OF PAPER CHEMISTRY
Appleton, Wisconsin

Status Report
to the
ENGINEERING PROJECT ADVISORY COMMITTEE

Project 3309
FUNDAMENTALS OF CORROSION CONTROL IN PAPER MILLS

March 23-24, 1989

PROJECT SUMMARY FORM

DATE: March 23, 1989

PROJECT NO.: 3309 - FUNDAMENTALS OF CORROSION CONTROL IN PAPER MILLS

PROJECT LEADER: Staff

IPC GOAL:

To increase the useful lifetime of equipment by proper selection of construction materials and by identifying suitable process conditions.

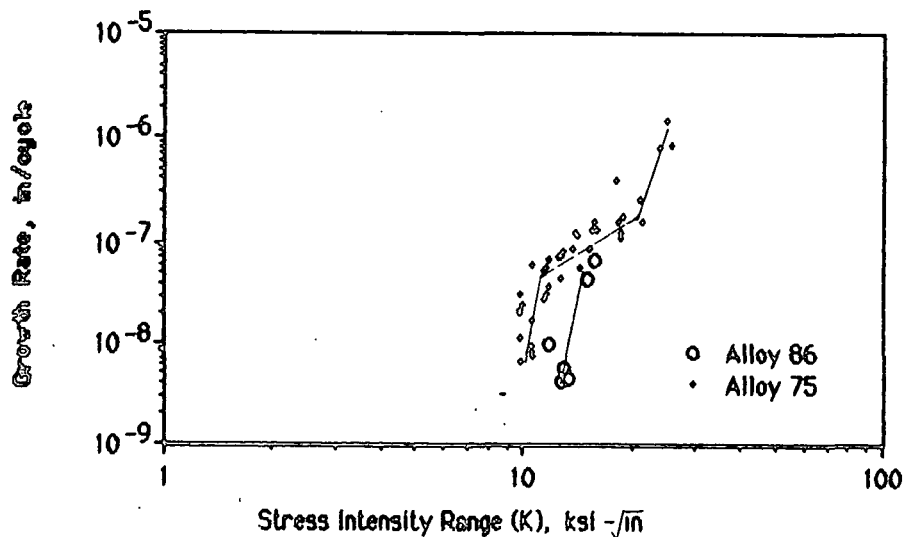
OBJECTIVE:

To increase the lifetime of paper machine suction rolls through corrosion and corrosion fatigue studies designed to establish the mechanisms that limit lifetime and to identify failure preventive measures.

CURRENT FISCAL BUDGET: \$150,000

SUMMARY OF RESULTS SINCE LAST REPORT: (September 1988 - March 1989)

Near threshold fatigue crack growth testing has been started on Alloy 86 using compact tension specimens in a test environment containing 1000 ppm Cl⁻ with the pH adjusted to 3.5. Limited preliminary results show the threshold stress intensity in Alloy 86 to be greater than that measured for the other alloys tested to date. A graph comparing the results of near threshold crack growth testing on Alloy 86 and Alloy 75 is shown below.



Comparison of the near threshold fatigue crack growth behaviors displayed by Alloy 86 and Alloy 75 in a 1000 ppm Cl⁻, pH 3.5 environment.

Rotating bar bending testing of Alloy 75 and Alloy 63 has been initiated in a simulated pit or crevice environment of saturated ferritic and chromic chloride solution with pH adjusted to 1 using HCl. At time of preparation of this report, runs in air have been done to provide a reference point for subsequent work.

Corrosion fatigue testing under tensile mean load conditions, using the Fatigue Dynamics "push-pull" machine, is in the planning stage. The push-pull testing apparatus has been delivered and is being fitted for testing under tensile mean load conditions. A suitable test specimen is being designed, as are grips usable in alternating tension and compression loadings, and a test solution containment chamber.

FUTURE PLANS:

1. Continue near threshold fatigue testing of current materials using new testing environments, formulated to simulate the composition of the electrolyte in a pit or crevice. Attempt to relate this data to cost per revolution of the suction roll. ?
2. Continue the rotating bending fatigue testing of Alloys 63 and 75 in a simulated pit environment saturated with ferric chloride and chromic chlorides with the pH adjusted to 1 with HCl. To date, the fully reversed loading S-N tests have been of little value in differentiating between suction roll alloys. If this work using a simulated pit environment does not provide results which distinguish between alloys, then this line of inquiry should be discontinued.
3. Extend the study of crack path through alloy microstructures in order to identify those metallurgical phases which are susceptible to rapid cracking, and those which may provide some degree of crack retardation in the materials tested in near threshold fatigue studies.
4. Investigate the microstructure of weld deposits on repaired suction rolls where filler metal has been added, especially for A75, A86 and VKA378. Results could be compared with the results of Task 3 to predict the possible effects of weld repair on fatigue life.
5. Investigate the effect of superimposed mean stresses on the crack initiation resistance of suction roll alloys in simulated white waters, to simulate residual stress effects.
6. Summarize the results to date in a report.

SIGNIFICANCE TO THE INDUSTRY:

The near threshold crack growth behavior has been shown to agree with service performance provided that residual stress effects are considered.

It has been confirmed that "cosmetic" welding, without post weld stress relief, will accelerate corrosion and stress corrosion in suction roll alloys.

THE INSTITUTE OF PAPER CHEMISTRY

Appleton, Wisconsin

Status Report

to the

ENGINEERING PROJECT ADVISORY COMMITTEE

Project 3470

FUNDAMENTALS OF DRYING

March 23, 1989

PROJECT SUMMARY FORM

DATE: March 23, 1989

PROJECT NO.: 3470 - FUNDAMENTALS OF DRYING

PROJECT LEADER: David Orloff

IPC GOAL:

Reduction of the "necessary minimum" complexity in number and/or sophistication of process steps.

OBJECTIVE:

To develop an understanding and a database sufficient for the commercialization of advanced water removal systems, based on high-intensity drying principles. This new technology will reduce capital costs, increase machine productivity, reduce the amount of energy used, and improve paper properties.

CURRENT FISCAL BUDGET:

\$150,000 from Institute funds, plus \$350,000 through a Department of Energy grant (as Project 3595). This grant is for a total amount of \$1.5 million over four years, this being the fourth of five budget periods for the project.

SUMMARY OF RESULTS FOR THIS REPORTING PERIOD: (September 1988 - February 1989)

During the current reporting period, we have concentrated our efforts on removing technical barriers to the commercialization of impulse drying for both heavy weight and light weight grades. Delamination of heavy weight grades, such as linerboard sheets, is the major hurdle to overcome. To achieve this objective, we are

working on three tasks: accumulating a delamination data base, developing a fundamental understanding of delamination, and investigating alternate platen designs that reduce or eliminate delamination.

Performance and Delamination Database

Based on limited experience, we suspected that the occurrence of delamination was a strong function of variables such as furnish characteristics, basis weight, and operating conditions. Some lightweight grades are relatively immune, while other grades are much more susceptible to delamination. We did not have the database required to define the range of acceptable operating conditions. Hence, we have examined several grades, weights, furnishes, as well as a range of operating conditions, to begin to define these boundaries.

The platen press has been a fairly good predictor of performance on the roll impulse dryer. The platen press is also much more productive and efficient as an experimental tool. For these reasons, the platen press was used for these studies, while future work will focus on verifying the results on the roll press.

Based on previous work by Lavery, we attempted to quantify delamination using the STFI compressive strength indexed to basis weight. For this purpose, two measurements were made from each of three 2.75 in. x 15 mm samples taken from impulse dried handsheets; an average STFI index was then calculated. A platen temperature vs. nip residence time map was used to record the STFI index for 159 gsm unbleached softwood kraft dried at a peak pressure of 450 psi, as shown in Figure 1. For these and all experiments reported in this paper, felt number 83516D was used. Also for all experiments where not specifically noted, the bottom platens were unvented. At a given platen temperature, increasing the nip residence time should result in either an increase or no change in strength as long as the sample does not delaminate. Hence, the conditions where the index first decreased was used as an indication of the onset of delamination.

**STFI INDEX- DELAMINATION WINDOW
UNBLEACHED SOFTWOOD KRAFT
(DRYER DESIGN #1)**

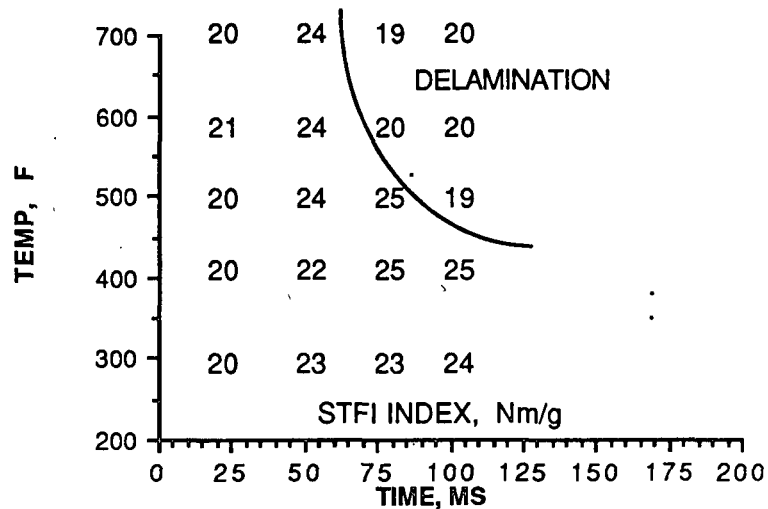


FIGURE 1

After obtaining additional data, the delamination region was mapped using visual observation to identify delamination. Three zones were identified. In the first zone, no delamination was observed. In the second zone, delamination ranged from complete sheet delamination to the presence of small blisters. The third zone, representing a transition between the two, showed delamination only on the edges of the handsheet.

Comparison of Figures 1 and 2 shows that visual observation was more conservative than the STFI index criteria in selecting the delamination region. However, both maps show that as the platen surface temperature was increased, the onset of delamination occurred at shorter and shorter nip residence times. This behavior is characteristic of the delamination process.

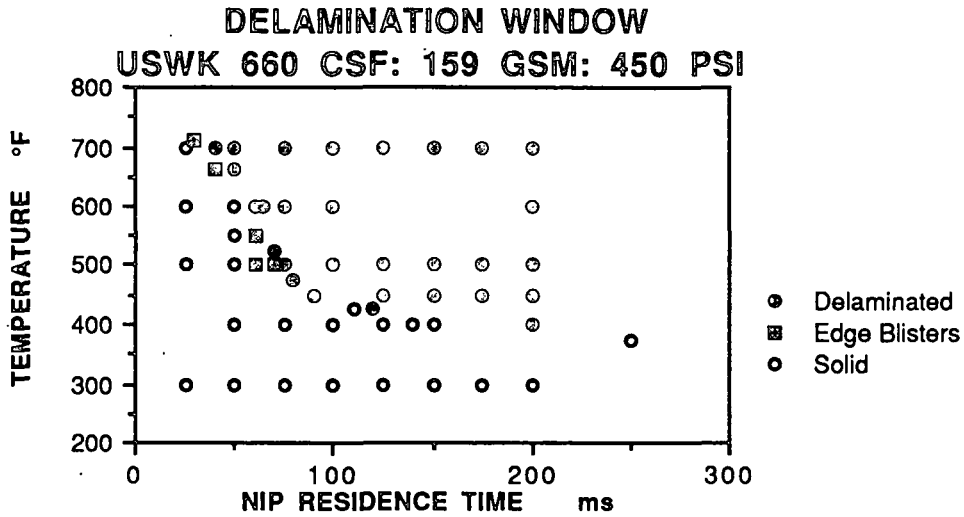


FIGURE 2

Focusing our attention on the 500°F data, STFI index plotted versus nip residence time is shown in Figure 3.

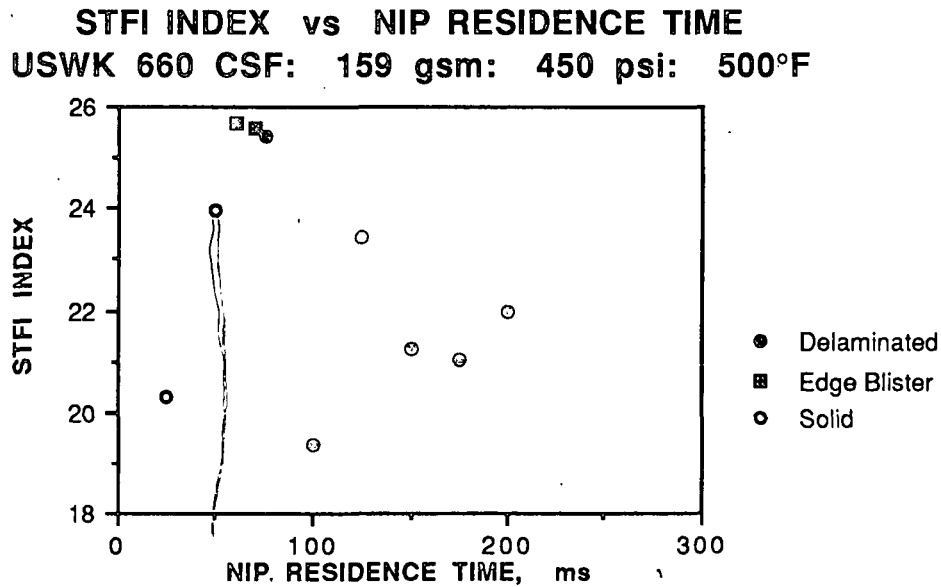


FIGURE 3

Clearly, samples that exhibit visual delamination can have high STFI. This was due to the fact that the STFI compression involves testing on a very small part of the specimen. Hence, if the specimen

was tested in an unblistered area, STFI strength will be high. We concluded that, for the purpose of identifying the delamination boundary, visual observation was preferred. Hence, visual observation was used in all subsequent work.

A series of experiments were run to determine the variables that most strongly influence the delamination boundary. For this work, we choose to examine a newsprint furnish and a 80% Eucalypt/20% Northern Softwood Kraft furnish. In all of these experiments, the initial sheet moisture was maintained near 30% solids and impulse dried at peak pressure of 450 psi.

The news furnish refined to 170 ml CSF and formed on the Formette Dynamique was evaluated for delamination at 50, 100 and 150 gsm. The basis weight of typical newsprint is approximately 50 gsm. At that basis weight and over a temperature range of 300-700°F and a 25-200 ms nip residence time range, no delamination was observed. At a higher basis weight of 100 gsm, delamination occurred as shown in Figures 4 and 5. Notice that in these, and subsequent figures, we have not distinguished between edge blisters and delamination. For these experiments, felt moisture was measured before and after impulse drying. Notice that the delamination window was virtually the same for the 2% and the 20% initial felt moisture cases. Intermediate initial felt moistures have not as yet been studied.

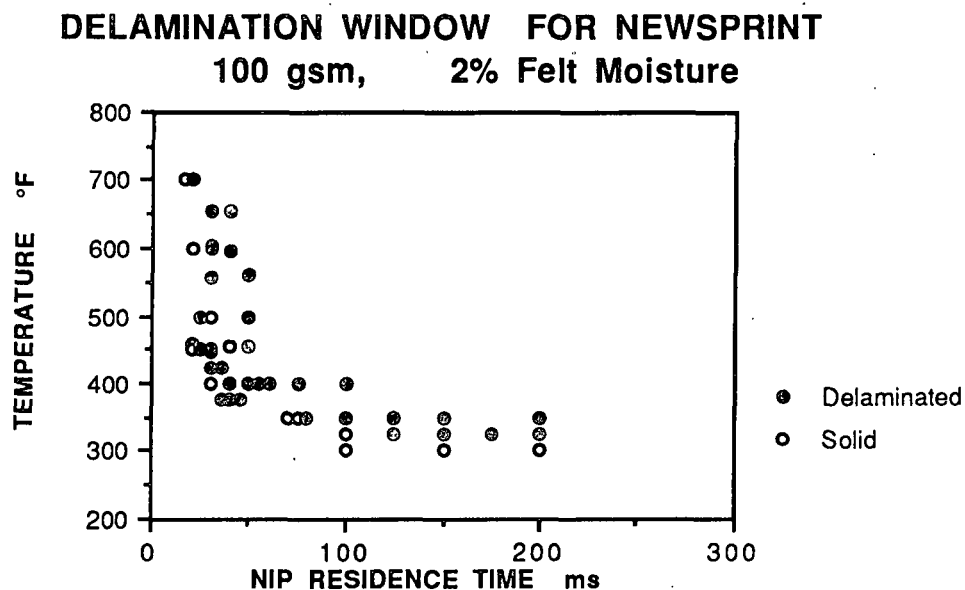


FIGURE 4

DELAMINATION WINDOW FOR NEWSPRINT

150 gsm 2.2 - 3.5% Felt Moisture

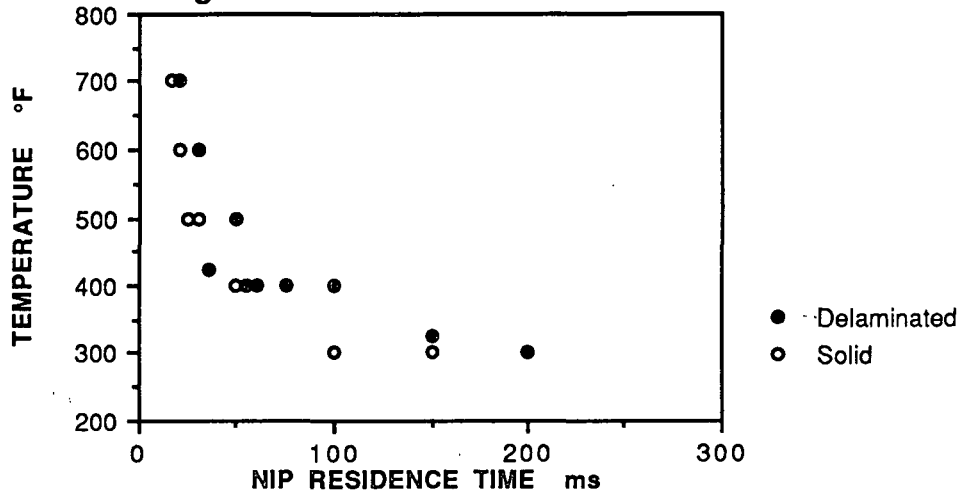


FIGURE 7

Figures 6 and 7 show that the influence of this difference in initial felt moisture on delamination was small. However, review of water removal rate data, shown in Figures 8 and 9, demonstrated a strong influence of initial felt moisture on water removal rates. This was especially true for the 150 gsm case.

WATER REMOVAL RATE FOR NEWSPRINT

100 GSM

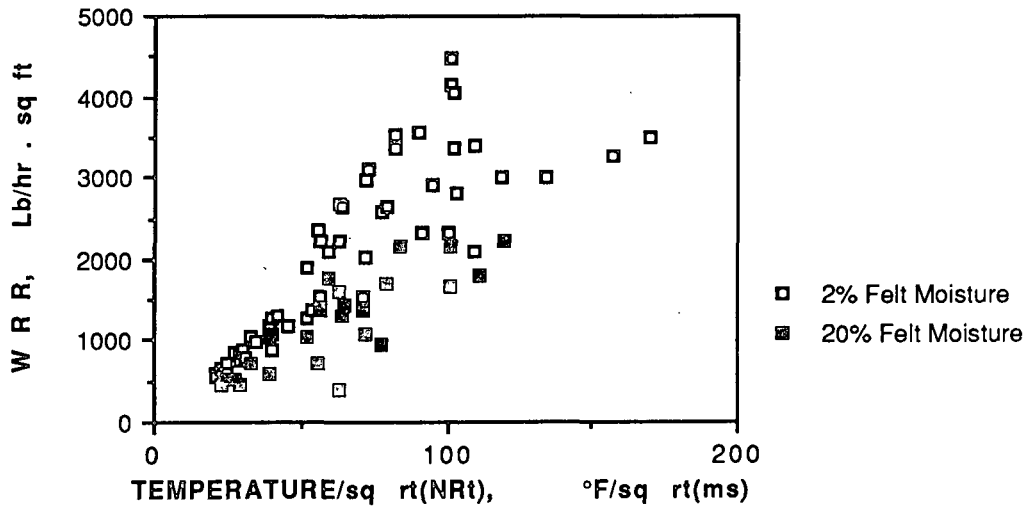


FIGURE 8

**WATER REMOVAL RATE FOR NEWSPRINT
150 gsm**

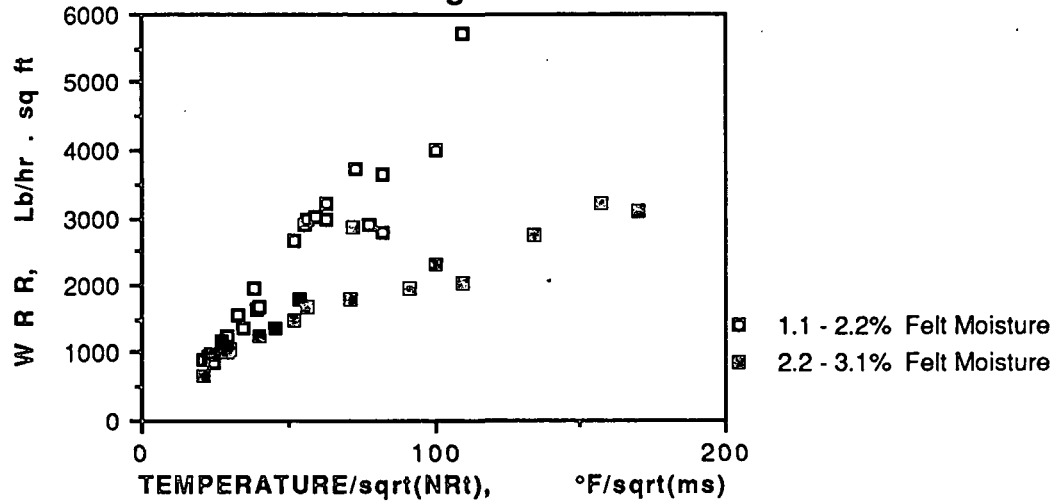


FIGURE 9

For comparison, the water removal rate for the Unbleached Softwood Kraft furnish is given in Figure 10.

**WATER REMOVAL RATE (NO DELAMINATION)
USWK: 660 CSF: 159 gsm**

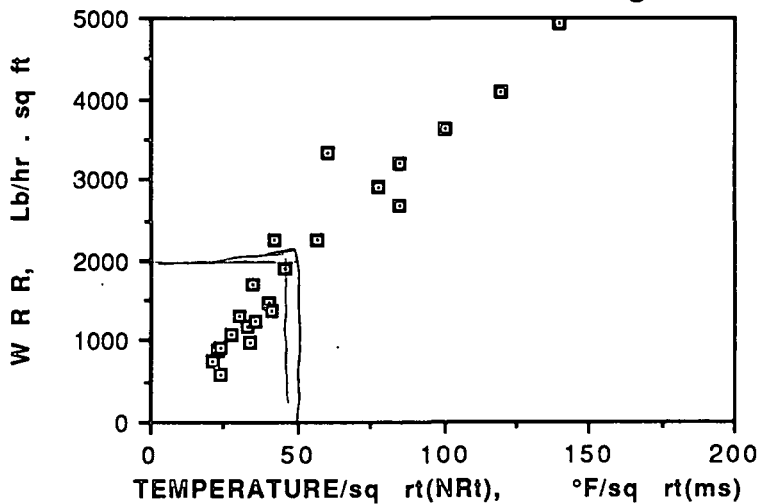


FIGURE 10

A blend of 80% Eucalypt and 20% Northern Softwood Kraft furnish refined to 296 ml CSF and formed on the standard British handsheet mold, was evaluated for delamination at four basis weight levels. Although there were limited data (see Figures 11 through 14), it appears that the operating window was more extensive for the lighter weight case than the heavier weight cases.

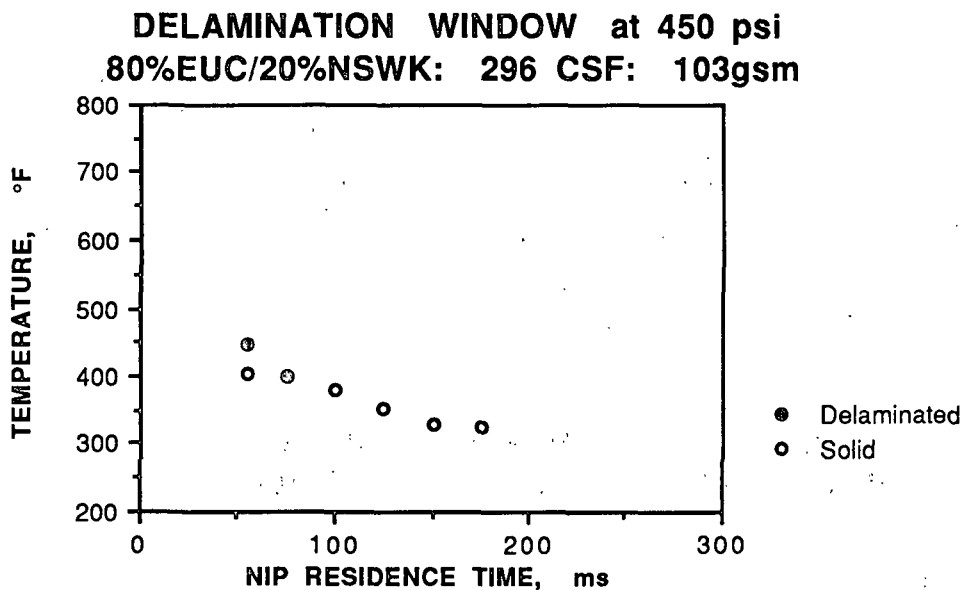


FIGURE 11

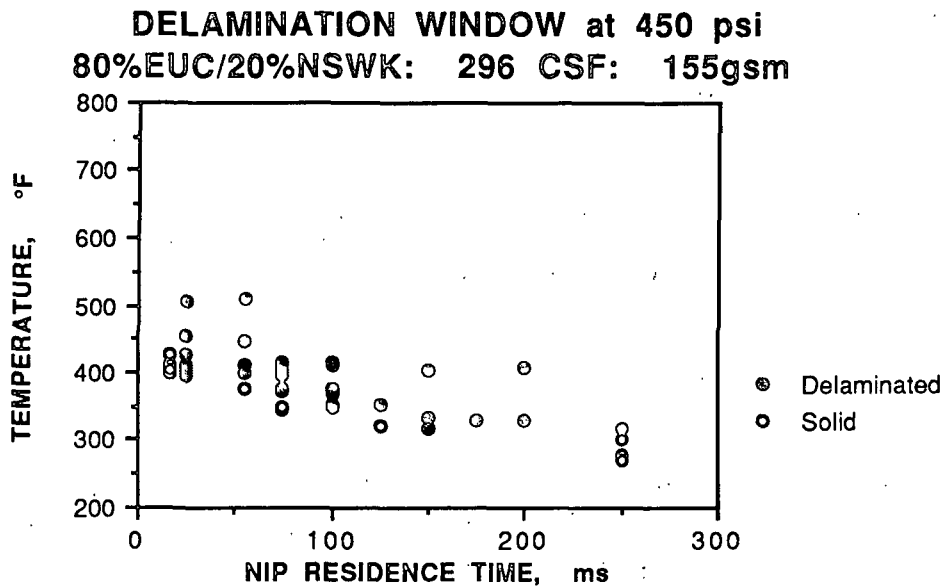


FIGURE 12

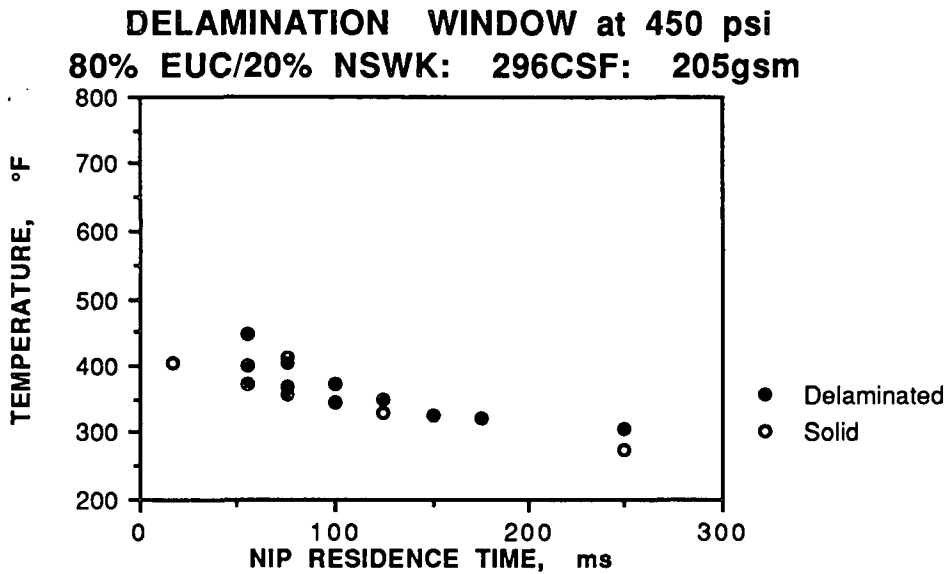


FIGURE 13

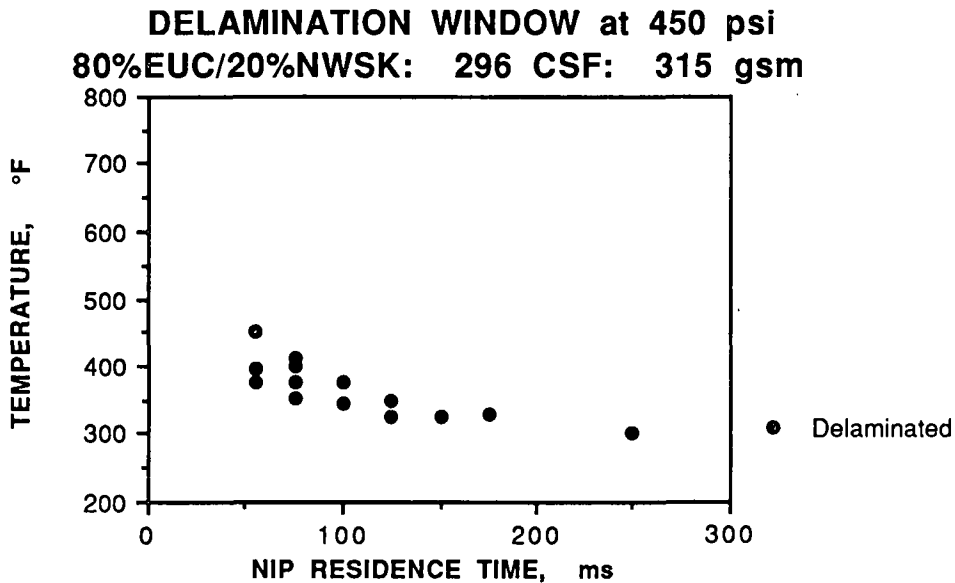


FIGURE 14

Comparing the delamination windows of the three furnishes presented shows that, at a comparable basis weight of 150-160 gsm, Newsprint and the Eucalyptus blend were similar while the Unbleached Softwood Kraft case exhibits a larger useful operating window.

Fundamentals of Delamination

*Effect of initial sheet temp?
on delamination?*

A second major part of our examination of the delamination question was the development of a more complete fundamental understanding of the mechanisms of impulse drying and delamination. Our concept of the process has been that of a time sequence of overlapping and intermingling events, including thermally augmented wet pressing, vapor displacement of liquid, and flash evaporation with attendant fiber dewatering and collapse. Vapor displacement is believed to be responsible for the rapid dewatering and excellent energy efficiency of the process. The rapid temperature rise through the sheet is believed to be the result of boiling heat transfer at or near the hot surface, and an internal evaporation-condensation-liquid reflux (heat pipe) type of heat transfer.

We hypothesize the following mechanism of delamination. As the sheet is heated under restraint in the early parts of the process, it stores energy in the form of superheated water. As the nip opens, water is permitted to flash by a reduction in pressure. Flashing releases energy at a very high rate, leading to overpressure and failure of the unrestrained and very weak sheet. We envision a vapor-liquid interface within the sheet, with some part of the liquid pool near the interface being superheated. Flashing would occur in this liquid pool, but near the interface. Since the sheet is still liquid-saturated at this point, it is very weak and susceptible to damage.

Our fundamental work was aimed at examining these concepts and their relationship to delamination. In particular, we examined the migration of temperature isotherms through the sheet. To do this, several thin but identical sheets were prepared. We first placed a thermocouple between a single sheet and the felt and impulse dried it to high solids level. The time when the temperature at this point first reached 212°F (or any other temperature level) was recorded. We then repeated the experiment with two such sheets, stacked one on top of the other. We also ran a separate experiment with a single sheet with the basis weight of the two.

We found that the time of arrival of the 212°F isotherm was the same for layered and solid sheets of the same basis weight. This was verified at the 90% confidence limit using the t test. This means

that the presence of the layers had no effect on the temperature history within the sheet. Hence, we could use thermocouples between layered sheets to determine isotherms during impulse drying.

Isotherms were measured for four furnishes. The time for the 212°F isotherm to pass through the sheet was then correlated to pressure (P), platen surface temperature (T), and sheet basis weight (BWT). The results are shown on Table 1, where the following correlation formula is applicable.

$$\text{Time (212°F)} = A + B(P/P^*) + C(T/T^*) + D(\text{BWT}/\text{BWT}^*)$$

Where; P*, T*, and BWT* are 100 psi, 300°F and 50 gsm respectively. and where ^{Time} P, T and BWT are given in units of ms, psi, °F and gsm.

TABLE 1

FURNISH	A	B	C	D
USWK	88.79	-0.689	-50.283	33.85
URO	112.48	-1.379	-69.430	43.15
E/N 460	76.85	-2.758	-40.793	31.15
E/N 300	86.95	+0.689	-68.432	58.15

Clearly pressure was a secondary effect as compared to temperature and basis weight. For ease of interpretation, the correlation was plotted for each furnish assuming a pressure of 450 psi and a basis weight of 100 gsm, as shown on Figure 15.

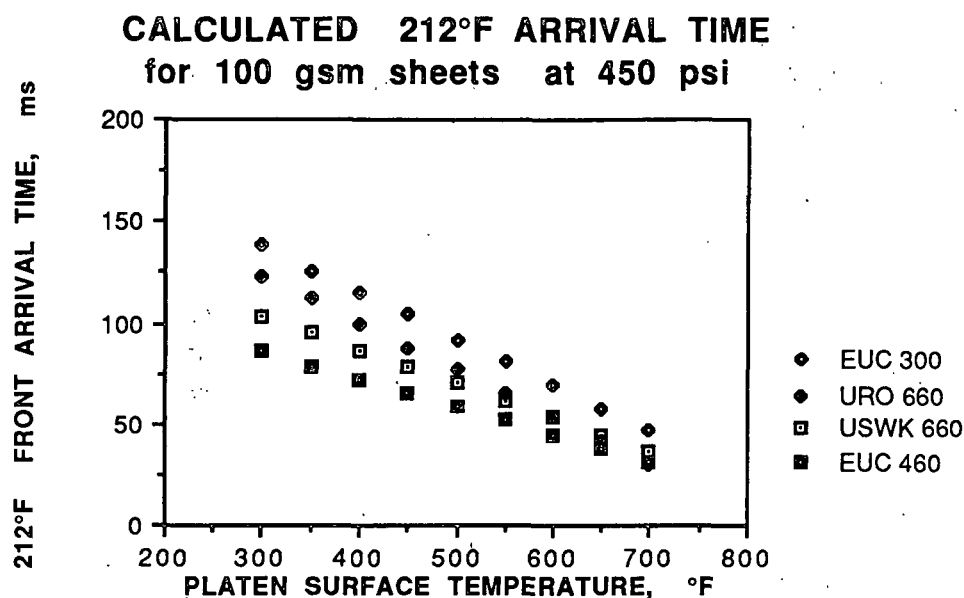


FIGURE 15

Refining had a significant effect on the speed of propagation of the isotherm, taken as the reciprocal of the arrival time. For the Eucalypt blend case, refining from 460 ml CSF to 300 ml CSF resulted in a decrease in speed by a factor of two.

A second set of similar experiments was designed to examine another aspect of the delamination concept. Here, single sheets of the same weight and furnish used in the first experiment were dried under conditions that produce complete delamination. From the respective weights of the two pieces of the split sheet, we were able to determine where delamination occurred in the z-direction. Here, "percent split from the hot surface" is defined such that 0 percent corresponds to the interface between the sheet and the hot platen, and 100 percent corresponds to the interface between the sheet and the cold platen.

The experiments were performed using the Unbleached Softwood Kraft furnish. The results are shown on Figure 16.

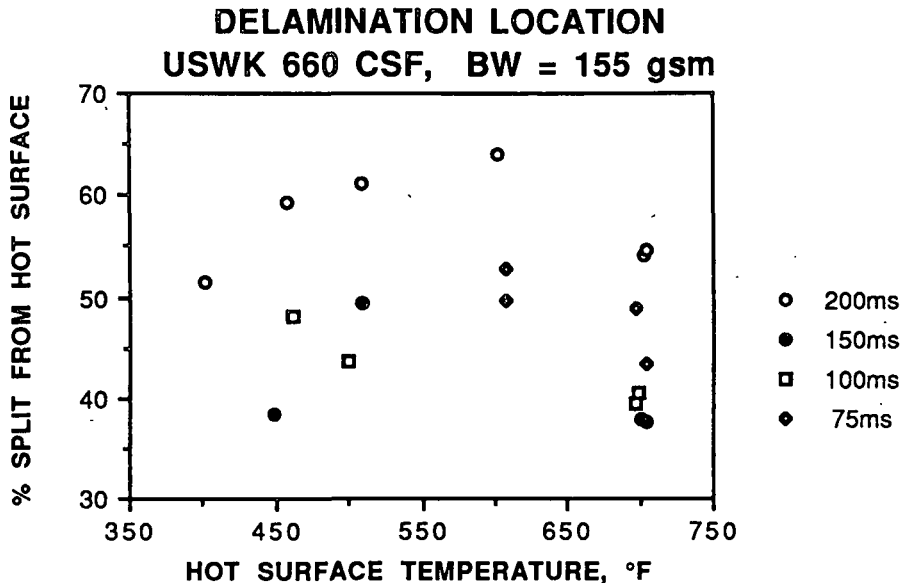


FIGURE 16

It was observed that the delamination zone was dependent on nip residence time and platen surface temperature. Low and high temperatures favor delamination near the upper heated platen. In addition, at a given platen surface temperature, long residence times favor delamination at the cold surface. This later result is consistent with our concept of a two phase front propagating from the hot platen to the cold platen.

To confirm our concept of the delamination mechanism, we need to demonstrate that, at a given platen temperature and as nip residence time increases, the process proceeds from a zone where there is delamination to a zone without delamination. These very long nip residence time experiments are in progress.

In a student project, Burkhead evaluated the effect of felt moisture on delamination for the case of a 60% BNHWK/ 40% BNSWK blend at a basis weight of 170 gsm. A haversine pressure pulse was used for these experiments. The premise of the work was that felt moisture and peak pressure influence delamination.

In the experiment, platen temperature was held constant at 450°F, while nip residence time was kept at 40 ms. Felt moisture ratio and peak pressure were varied to observe their influence on delamination. The work showed that delamination was more likely to

occur at either very low or very high felt moisture ratios. Burkhead also found that, independent of felt moisture ratio, delamination always occurred above peak pressures. In additional work, Burkhead plans to investigate the effect of initial moisture and pressure on felt permeability.

The practical consequences of Burkhead's work are that both pressure and felt moisture profiles may need to be carefully controlled on the pilot impulse dryer to eliminate delamination. The extent to which they must be controlled was the subject of additional experimentation. Using Unbleached Softwood Kraft furnish, we investigated the influence of felt moisture and pressure at 550°F surface temperature at 50 and 100 ms. We used a vented-bottom cold platen to simulate the first nip of our pilot impulse dryer. As a baseline case, we developed a delamination boundary where basis weight and nip residence time were variables. Figure 17 shows that, at 450 psi and 20 percent initial felt moisture, delamination occurred at basis weights above 150 gsm and at nip residence times longer than 100 ms.

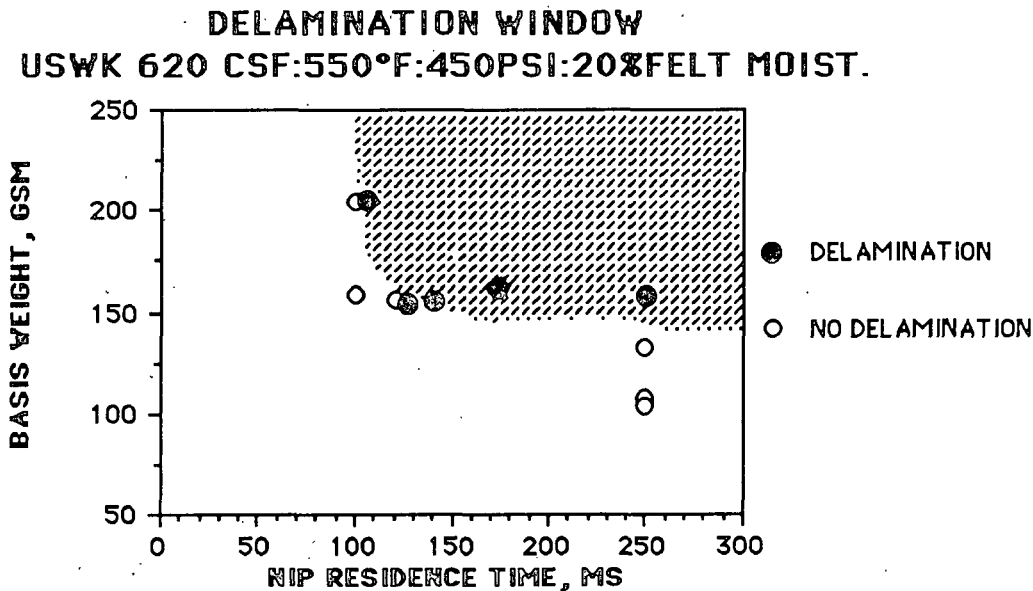


FIGURE 17

Experiments using 127 gsm sheets showed no delamination at either 50 or 100 ms in a range of initial felt moisture of between 2 and 35 percent, and in a range of pressures between 200 and 650 psi. As shown in Figures 18 and 19, experiments using 205 gsm

sheets demonstrated that the effect of peak pressure on delamination was dependent on nip residence time. Interestingly, we did not see the influence of initial felt moisture that Burkhead observed. As there was only one test per condition, replications are planned in order to define the boundaries more accurately.

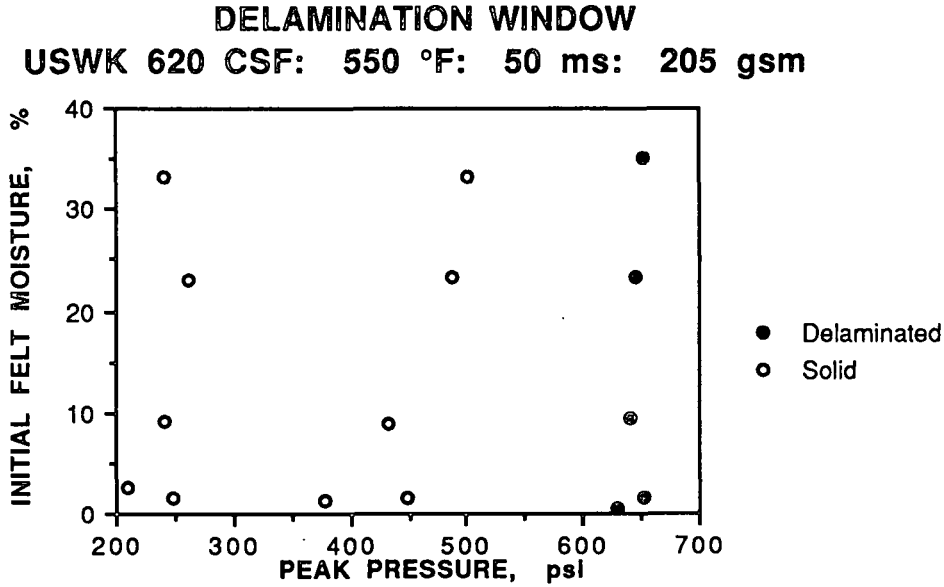


FIGURE 18

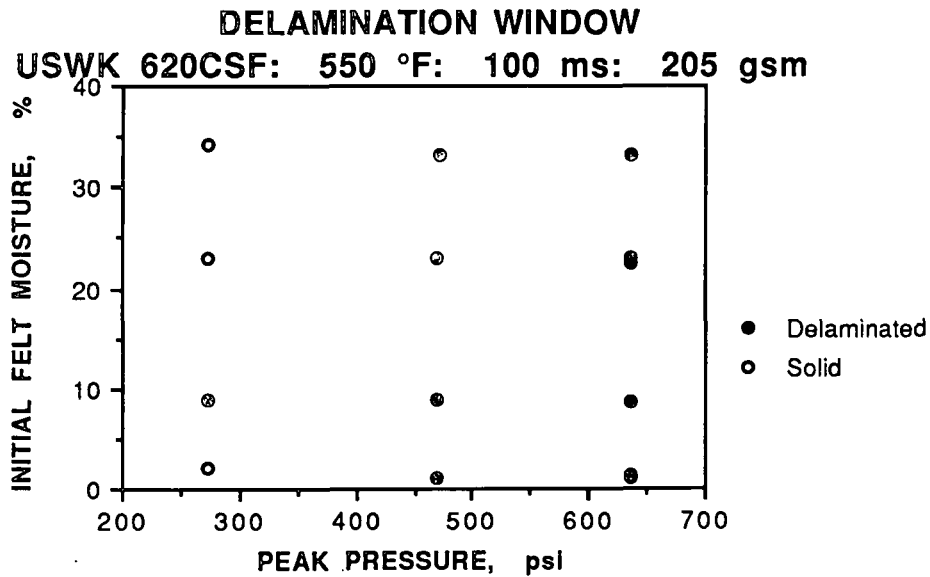


FIGURE 19

Alternate Implementation Systems

If the concept of delamination is correct, more heat energy is supplied to the sheet than can effectively be used for water removal, with the result being delamination. This leads to the consideration of alternate implementation systems.

An approach to alternative systems was to examine heat addition to the sheet. To this end, we have investigated in an exploratory experiment, several different heated surface configurations which cover a range of heat transfer parameters.

For these experiments, a system for quickly interchanging heat transfer surfaces was designed and constructed. Several types of surfaces were available for testing. To test these, a furnish-weight combination that experienced delamination in a typical operating range was selected. The influence of these alternate surfaces on the location of the delamination boundary was examined.

As part of a student project, Santkuyl performed experiments with platens fabricated from a number of materials. These included two solid platens; one of steel and one of an aluminum alloy. In addition, platens made from sintered stainless steel, at two different porosities, were evaluated. Considering transient heat flow in a semi-infinite solid, the heat flux from the platen to the paper is proportional to $(\rho * C_p * k)^{1/2}$. This factor was virtually independent of temperature and is given for each of the platen materials in Table 2.

TABLE 2

<u>PLATEN MAT'L</u>	<u>$(\rho * C_p * K)^{1/2}$</u>
Solid Aluminum	2.2
Solid Steel	1.4
Low Porosity Steel	0.35
High Porosity Steel	0.25

Delamination boundaries were evaluated for samples produced from the Unbleached Softwood Kraft furnish refined to 640 ml CSF at a basis weight of 215 gsm. Samples were made on the Formette Dynamique to optimize formation. In these experiments, Santkuyl

found evidence that the aluminum platen had a more extensive delamination boundary than the steel platen at 700°F and 60 ms. However, in repeating these experiments at temperatures below 650°F, we observed a slightly less extensive delamination boundary on the samples impulse dried with the aluminum platen. See Figures 20 and 21.

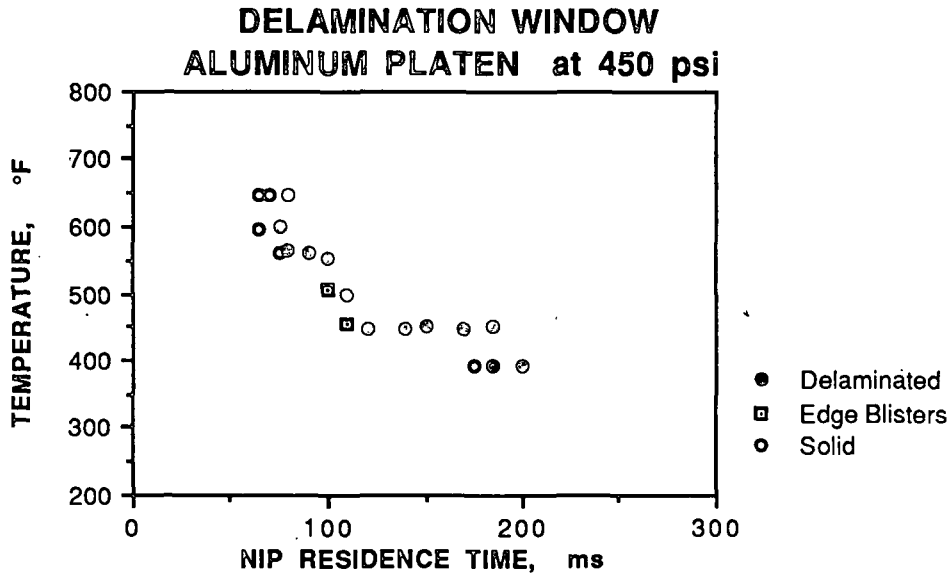


FIGURE 20

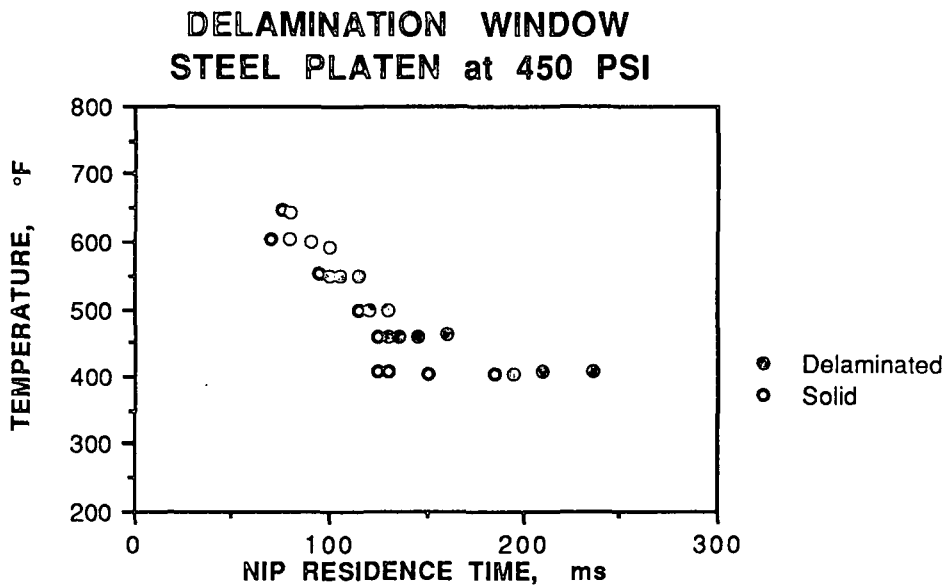


FIGURE 21

Using porous stainless steel platens, Santkuyl found no evidence of delamination over the range of process conditions investigated for the solid aluminum and steel platens. It was noted, see Figure 22, that the strength of nondelaminated samples was independent of platen material for a given sheet density, as measured using the C33 ultrasonic modulus.

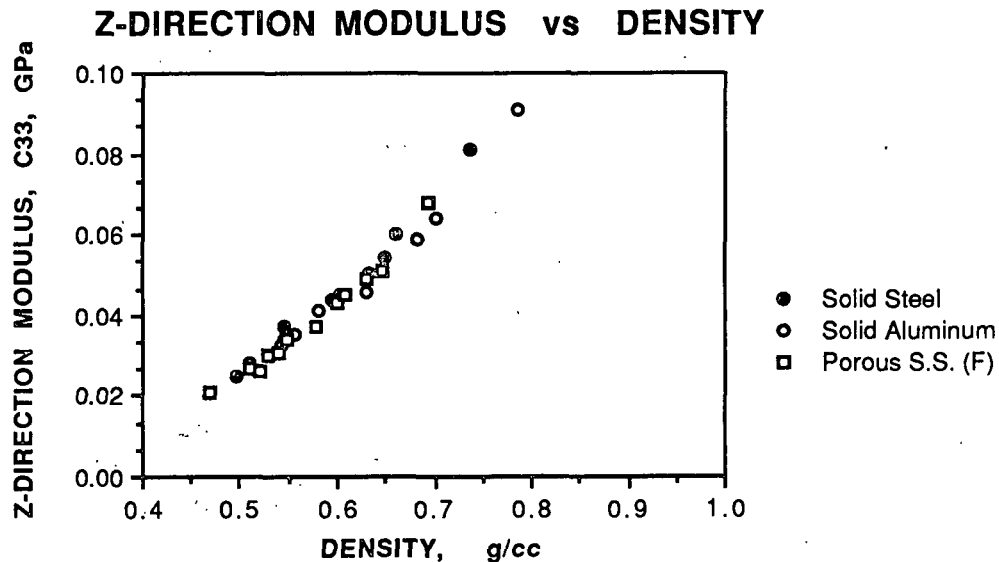


FIGURE 22

However, as shown on Figure 23, the sheet density produced using the porous platen was slightly lower than that produced by the steel and aluminum platens at the same percent solids.

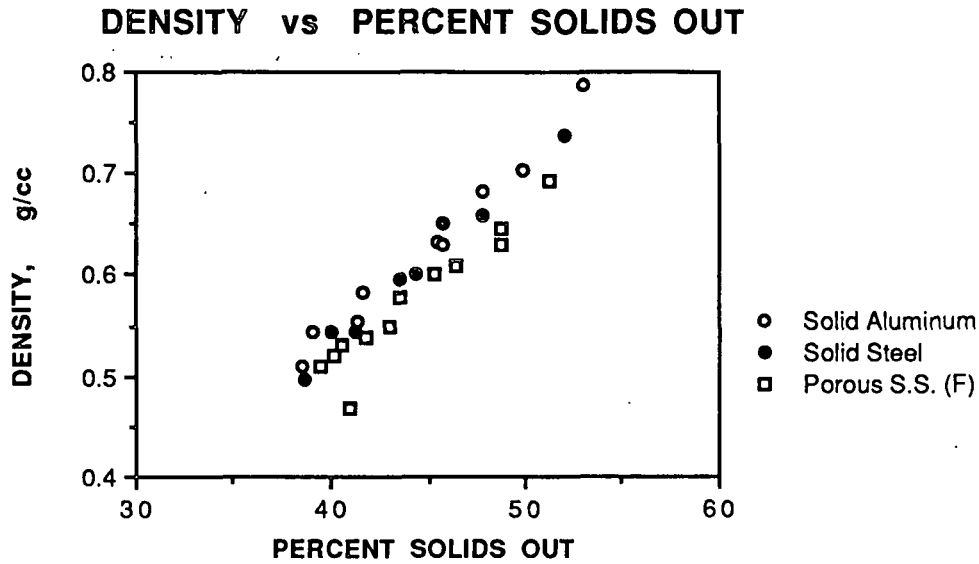


FIGURE 23

We found that water removal rates for the aluminum and steel plates were similar, even though they were made of materials with significantly different $(\rho \cdot C_p \cdot K)^{1/2}$. See Figure 24. This seems to imply that process drying rate is independent of the rate of heat flux through the platen.

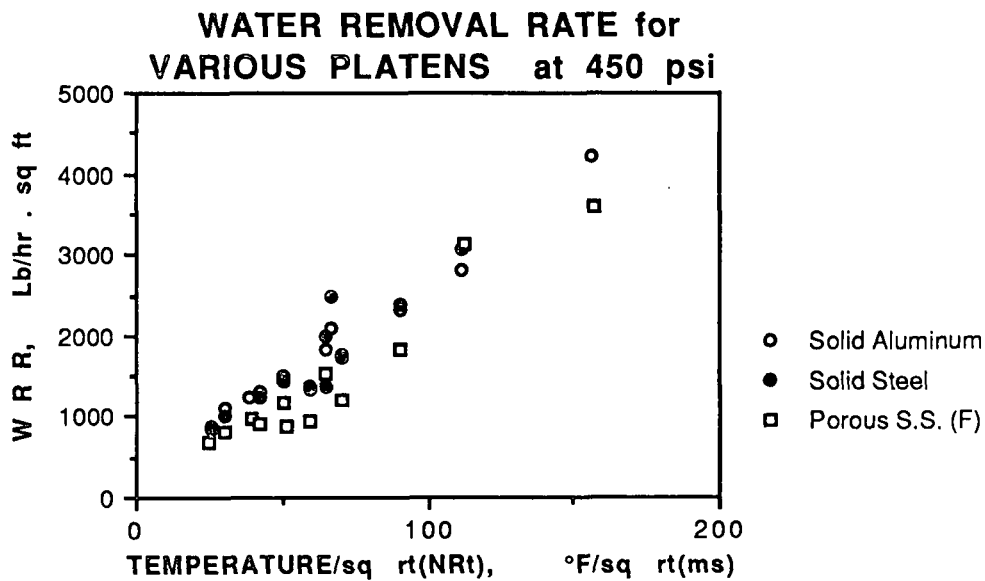


FIGURE 24

Water removal rates for the porous platens were slightly lower than those of the solid platens. Hence, at similar operating conditions, the porous platens yielded a slightly lower percentage of solids out than the solid platens.

In a set of exploratory experiments, temperature histories were measured during impulse drying of sheets formed from Unbleached Softwood Kraft. Impulse drying conditions were set at a pressure of 450 psi and a platen surface temperature of 500°F. In addition to the solid steel and aluminum platens, stainless steel platens with fine and coarse pores were also tested. Figure 25 shows the temperature response of thermocouples located between the sheet and the felt.

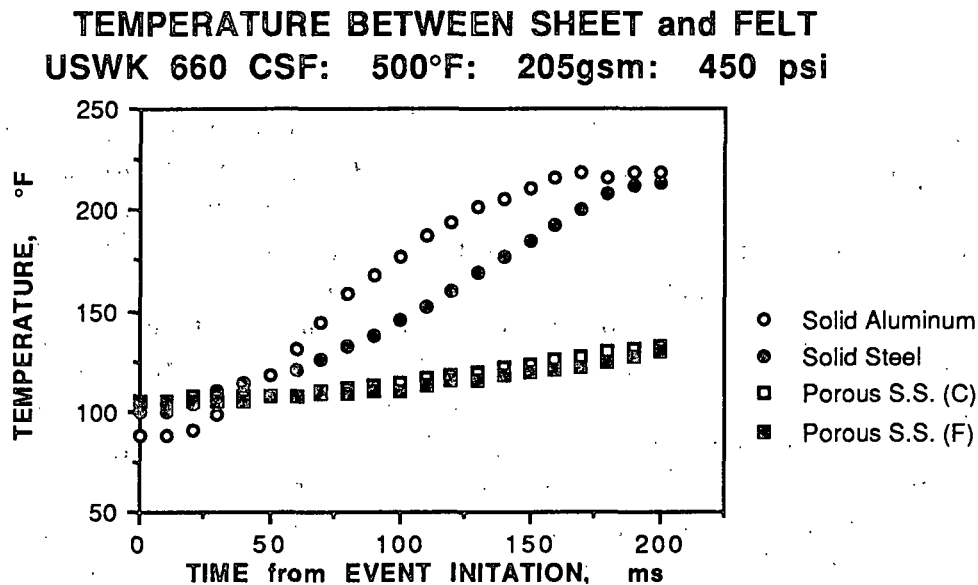


FIGURE 25

Consistent with our expectation of the effect of platen thermal properties on heat flux from the platen, the aluminum platen showed a faster temperature rise than the steel platen, while the porous platens showed an even slower temperature rise. Hence, we might draw the conclusion that reducing heat flux below a threshold level eliminated delamination. Analysis of weight loss data, shown on Figure 26, suggests another possible explanation.

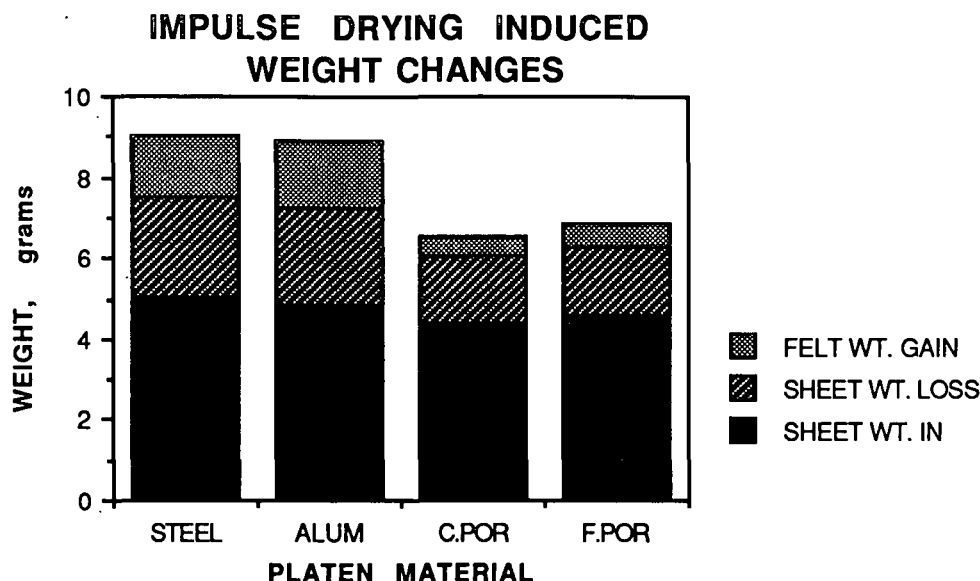


FIGURE 26

Clearly, the sheet weight loss for the solid platen experiments was greater than that of the porous platens. This is consistent with Santkuyl's results. Yet the weight gain of the felts in the porous platen case are significantly lower than that of the solid platens. A plausible explanation is that steam formed during the process is partly vented through the porous platen. This would not only explain the lower weight gain of the felt, but would also explain the slower temperature rise observed for the porous platen case. The question remains whether the difference in delamination between solid and porous platens is due to a lower heat flux, venting, surface characteristics, or some combination of all three. Resolving this issue will be a major task in future work.

Summary

Considerable new knowledge has been obtained on: the extent, the mechanism, and the means to avoid delamination during impulse drying.

1. We have found that the following variables influence the occurrence of delamination; furnish, refining, basis weight, felt moisture, temperature, nip residence time, and peak pressure. Delamination windows determined on the MTS suggest that operating

conditions exist where heavy weight sheets can be dewatered without delamination.

2. Temperature profiles and determination of the z-direction locations of delamination has increased our understanding of the delamination mechanism. We now know that the sheet delaminates closer to the felt as the nip residence time increases.

3. Experiments showed that, for solid platens, process drying rate is independent of the heat flux from the platen. We have also found that delamination can be controlled, at all operating conditions, through the use of porous heated surfaces. Although the mechanism is unclear, early results indicate that sheet physical properties are not adversely affected. Depending on the importance of steam venting to the operation of the porous surfaces, energy efficiency may suffer.

Plans for The Next Period

1. Determine the mechanism by which the porous platens operate. We need to resolve whether steam venting, surface characteristics or reduced heat flux is the dominant mechanism. The following questions need to be answered.

- If delamination suppression is dependent on heat flux, is there a threshold?
- If venting is important, what is the minimum required, and what is the impact on energy usage and property development?
- If surface characteristics are important, would a solid platen with the same characteristics produce similar results to the porous platens?

2. Based on our hypothesis that control of heat flux is important to delamination control, we plan to investigate platens made of composite materials. The concept is to deliver a high heat flux during the compression part of the nip and then a decreasing heat flux during the expansion part of the nip.

3. Continue development of the delamination database and fundamental work that will lead to an understanding of the delamination mechanism. Compare delamination boundaries at similar conditions on the MTS and the pilot impulse dryer (EHRID).

4. Develop a performance database for several lightweight grades that are insensitive to delamination including: newsprint, lightweight coating rawstock, and writing paper. The database will consist of information relating impulse drying process variables to drying performance and product properties.

References

Burkhead, J.R., Effect of Felt Properties on Delamination During an Impulse Drying Event, A190 Project, The Institute of Paper Chemistry, 1989.

Lavery, H.P., High-Intensity Drying Processes-Impulse Drying Report Three, DOE/CE/40738-T3, The Institute of Paper Chemistry, February 1988.

Santkuyl, R., Effect of Surface Material on Delamination in Impulse Drying, A190 Project, The Institute of Paper Chemistry, 1989.

THE INSTITUTE OF PAPER CHEMISTRY
Appleton, Wisconsin

Status Report
to the
ENGINEERING PROJECT ADVISORY COMMITTEE

Project 3480
FUNDAMENTALS OF WATER REMOVAL PROCESSES

March 23-24, 1989

PROJECT SUMMARY FORM

DATE: Feb. 28, 1989

PROJECT NO.: 3480 – FUNDAMENTALS OF WATER REMOVAL PROCESSES

PROJECT LEADER: Jeff Lindsay

IPC GOAL:

Develop novel processes for efficient water removal with enhanced control over paper properties.

ABSTRACT

New progress has been made in the numerical modeling of displacement processes such as impulse drying. While the focus of recent activity has been on the modeling of impulse drying, the numerical tools can also be adapted for a variety of displacement processes where heat transfer is important. Modeling tools for isothermal displacement have also been developed which treat two-phase flow issues at a much higher level of sophistication than is currently practical for impulse drying.

The experimental work in displacement dewatering has been stalled due to excessive demands on the MTS electrohydraulic press. Dues-funded and contract research involving impulse drying have made the equipment unavailable during the last 6 months. No relief appears to be in sight, although other options are being explored.

The study of anisotropic permeability has been hindered by the demands on the MTS system as well, but a Carver press is now being modified to permit a

continuation of this study. A separate student project was recently found to have relevance to the lateral permeability of paper; a collaborative effort is now underway to apply new numerical tools to extract anisotropic permeability data from the student's measurements.

REVIEW OF RECENT PROGRESS

Experimental Investigation of Displacement Processes

Direct Displacement Dewatering

Direct displacement dewatering, in which a pressurized gas phase is directly applied to a compressed sheet, has been a focus of this project in the past. Experimental equipment was designed and constructed, and preliminary tests were made, as reported in the last PAC report [1]. Unfortunately, the experimental work in displacement dewatering during the last period has been stalled due to constant demands on the MTS electrohydraulic press for impulse drying studies. Other options have been explored, but no satisfactory solution appears to exist at this time, although two weeks of experimental time with the MTS have been scheduled prior to the move to Atlanta. After the move, there is the likelihood of access to other MTS systems on the campus of Georgia Tech, and the possibility of decreased demands on the MTS system owned by the IPC.

While experimental work in direct displacement dewatering has been hindered, experimental and numerical investigations of related displacement processes have continued, as described below.

Impulse Drying

An improved understanding of impulse drying physics is believed to be of value in understanding other displacement processes, especially those in which heat transfer might be a factor. For this reason some fundamental aspects of impulse drying physics have been pursued, supplementing some of the research done under Project 3595.

The Role of Pressure: Impulse Drying vs. Wet Pressing

Displacement is believed to be a key factor in impulse drying. If displacement does occur, the relation between sheet compression and displacement velocity becomes of interest. As a sheet is compressed, its permeability decreases, making displacement more difficult. On the other hand, the decreased thickness of the sheet increases the pressure gradient, partially compensating for the lower permeability. In impulse drying, improved thermal contact at higher mechanical pressures may improve heat transfer and further compensate for the lower permeability.

To explore these effects, a study was conducted in which water removal by wet pressing and impulse drying was examined as a function of applied pressure. The study used several batches of linerboard handsheets with 250 g/m² basis weight and solids contents near 35%. Impulse drying was done at 260°C. The MTS hydraulic press system was used with a haversine pressure pulse and a nip residence time of 30 milliseconds. Care was taken to maintain constant felt properties and to use randomization with respect to felts and sheets. Both handsheets and felts were weighed before and after the pressing events to track the water flow.

Typical results are shown in Figure 1, where the peak pressure is varied from 600 to 1600 psi. The water removal data are reported as mass of water removed divided by the initial sheet weight. The difference between the wet pressing and impulse drying curves represents the extra water removed by impulse drying. Interestingly, the amount of extra water removed does not seem to decrease with increasing pressure over the range investigated. The results of Figure 1 were replicated in two other batches of handsheets, and the same trend was also observed over the pressure range of 200-600 psi in other linerboard handsheets. (In one case, the extra water removed by impulse drying appeared to increase with increasing pressure, rather than remain constant.)

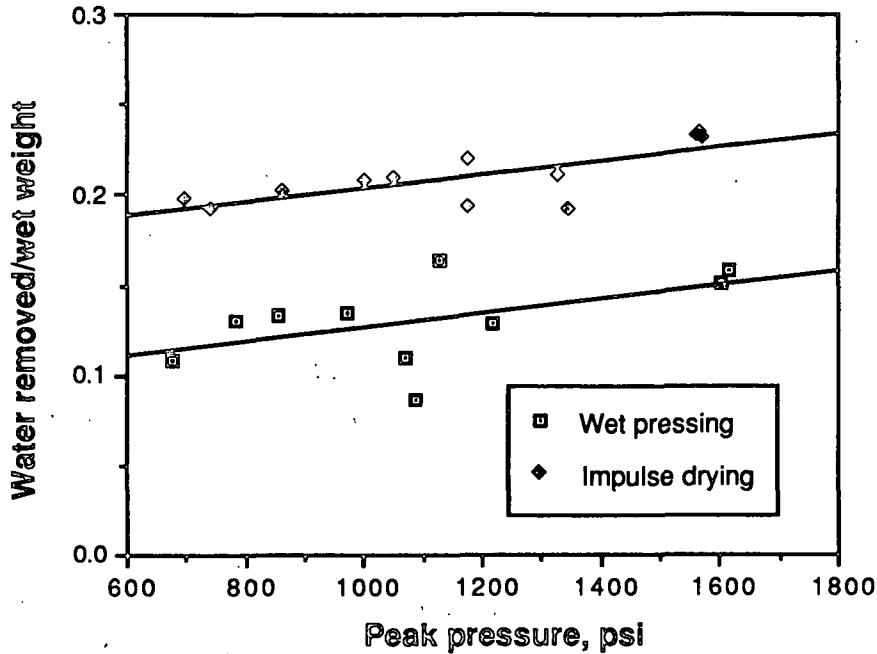


Figure 1. Comparison of water removal in wet pressing and impulse drying as a function of pressure. 250 g/m² linerboard handsheets were used. Impulse drying temperature was 260 °C.

The extra water removed by impulse drying would be nearly constant if it were all due to vaporization, but the measurements of water added to the felt show that about 90% of the extra water removed is in liquid form (the possibility of steam breaking through the 250 g/m² sheet and condensing in the felt is easily ruled out by an examination of felt surface temperature in related measurements). This is consistent with the energy balance and mass balance measurements made by Lavery [2-3] and contradicts a recent speculation [4] that the heat flux into the sheet simply provides energy to evaporate the water, and that the gain of impulse drying over wet or hot pressing is due to evaporative removal alone.

The small pressure-dependency in the extra water removed by impulse drying may be due to several factors compensating each other, as discussed above. But it also raises the possibility that a mechanism with less pressure dependency than displacement may be contributing to the extra water removal found in impulse drying. Such a mechanism might be rewet reduction, as discussed below.

Rewet Reduction by Impulse Drying

The recent modeling results of this study [5,6] along with the physical observation of delamination both suggest that significant vapor pressures can exist throughout the entire pressing event, and that these pressurized vapor zones are not just confined to the upper surface of the sheet. With a pressurized vapor region already in the sheet, the normal process of rewet may be greatly reduced or reversed in impulse drying. This contribution to liquid water removal in impulse drying has apparently not been considered before, but may be of importance. The hypothesis is thus advanced that the enhanced liquid water removal obtained in impulse drying is indeed due to the presence of a pressurized vapor phase, but that the mechanism must include both displacement and rewet reduction. The pressurized vapor zone is expected to reduce rewet by suction, capillary forces, and film splitting. Student research on this possibility is currently underway [7]. If rewet reduction plays an important role in impulse drying, it can also be expected to be of benefit in direct displacement dewatering.

Flash X-ray Visualization (Student Research)

During the last period many tests have been conducted using flash x-ray radiography to visualize the steam-water interface which may form in impulse drying [8]. The technique tracks the motion of an x-ray-absorbing silver nitrate tracer solution added to the upper layers of a linerboard sheet. Impulse drying and wet pressing events were approximated with a falling-weight press-nip simulator. During the pressing event, a brief burst of x-rays was sent horizontally through the sheet and the felt, as shown in Figure 2. The location of the silver nitrate solution in the z-direction could be observed in the radiograph. Different delay times are used in each run, allowing fluid motion to be observed in time.

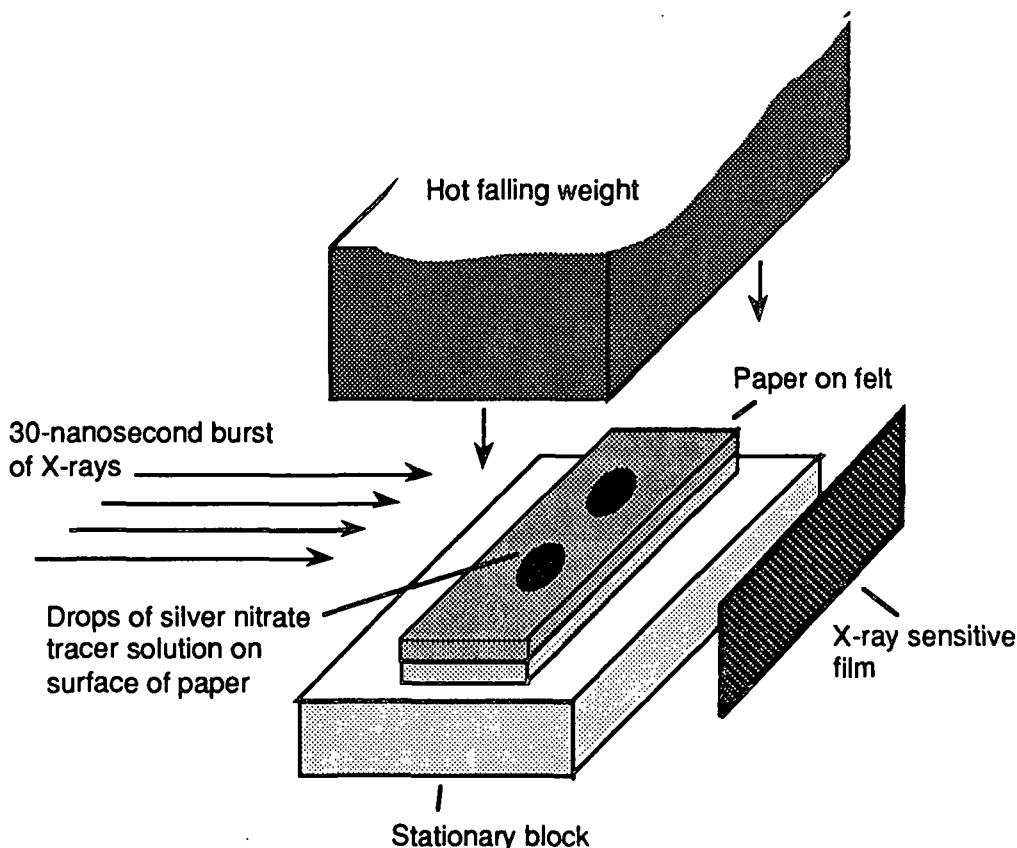


Figure 2. Experimental configuration for flash x-ray visualization of liquid motion in impulse drying. The location of tracer solution in the vertical direction can be viewed during any part of a pressing event.

Recent radiographs taken under realistic impulse drying and wet pressing conditions do show what appears to be a vapor zone in the paper next to the hot metal surface. (Similar preliminary results were reported in the previous report [1], but the applied mechanical pressure was much higher than would occur in a practical operation.) The vapor zone is not clearly visible until after the peak in the pressure pulse, and never extends beyond roughly 10-20% of the sheet thickness. If the observed vapor zone indicates the extent of displacement achieved in impulse drying, it may not be great enough to account for the enhanced water removal which occurs. While the observed low density region probably represents a dry zone, a larger two-phase zone containing both liquid and steam may be present which is not distinguishable from a saturated zone without further improvements in the experimental method. Again, the presence of a vapor zone may also lead to enhanced water removal by rewet

reduction, apart from displacement by the vapor zone. In any case, the existence of a vapor zone and the motion of fluid through a sheet can be observed with the flash x-ray technique. This method is now also being applied to impulse drying in a small roll press [9].

Numerical Modeling of Displacement Processes (Impulse Drying)

Previous numerical modeling resulted in a model, MIPPS-I, for the moving boundary problem of thermally-driven displacement in a rigid porous medium. The model assumed a sharp steam-water interface whose temperature, pressure, and position changed in time. The model, while deficient in a number of details, provided several insights into the phase-change heat transfer process of impulse drying [5,6]. One of the conclusions obtained with MIPPS-I was that the experimentally measured heat transfer rates could not be explained unless liquid was continually boiled near the surface, even after displacement had moved the saturated liquid zone (the steam-water interface) far away from the surface. A mechanism of capillary resupply was then proposed. A capillary resupply mechanism, however, contradicts the assumption of a sharp steam-water interface. In addition, some recent experimental measurements of temperature propagation in layered sheets have implied the presence of a two-phase zone in at least some cases. An improved numerical model, in which a two-phase zone is possible, was therefore pursued.

Model Development

Examination of MIPPS-I predictions eventually revealed that several factors in the model were not important, suggesting useful simplifications for MIPPS-II. The pressure drop in the gas phase, for instance, was shown in the predictions to be small enough to permit the assumption of spatially uniform gas pressure (although the pressure changes in time). Non-Darcian terms in the momentum equations were also found to be unimportant, and have thus been dropped in MIPPS-II. These simplifications made it possible to introduce a more complicated treatment of the steam-water boundary, replacing a sharp interface with a broad two-phase zone.

MIPPS-II allows a two-phase zone to form as gas displaces liquid. It is assumed that the moving liquid zone leaves behind a fraction of the previously present liquid. This can be due to capillary forces, trapped pores, and the effects of relative permeabilities [10,11]. In the absence of detailed experimental data for trapped pore volumes, non-equilibrium capillary pressure functions, and relative permeability, the liquid in the two-phase zone is treated as if it were due to trapped pores only, and a constant remaining saturation, S_r , is specified to describe what fraction of the initially saturated liquid is left behind in trapped pores as the saturated liquid zone recedes. Because the remaining water is assumed to be trapped once it is left behind, at least for the time scale of the displacement process, it has a relative permeability of zero and will remain in place until it has evaporated. If the saturated liquid zone moves away faster than the beginning of the two-phase zone is evaporated, the two-phase zone will grow in time. Likewise a high heat flux can cause the zone to shrink.

While this approach does not require a specified capillary resupply rate which was needed in MIPPS-I, it does introduce another parameter, S_r . This factor, however, is more closely related to the inherent physical nature of the sheet than is a resupply rate. For a given sheet, S_r is expected to be a function of compression and temperature, but a constant is used as a mask for ignorance. Based on general information about wet pressing and flow in fibrous porous media, it appears that S_r could be on the order of 0.1 to 0.4, but this is largely a guess at this point.

The steam and liquid water in the two-phase zone are at equilibrium. Since the pressure drop in the gas phase is assumed to be negligible, the equilibrium conditions require the two-phase zone to be at constant temperature.

With this framework, transport equations for heat transfer and fluid flow in the porous medium can now be applied. The equations used are similar to those from which MIPPS-I was derived, with some simplifications. A thermodynamically-sound procedure for maintaining equilibrium in the two-phase zone was implemented. The complete details of the model are given in [6].

Boundary conditions are similar to those of MIPPS-I, with the added complication that phase change can occur at the beginning and the end of the

two-phase zone due to differences in thermal conduction, and phase change can occur throughout the entire two-phase zone to maintain equilibrium. The initial condition assumes that a thin dry layer and a thin partially-saturated layer exist at the top of the sheet (all initial conditions are specified by an input data file for each run, and are not built into the code).

The key equations for MIPPS-II were discretized into explicit finite-difference forms using a moving, staggered grid with uniform grid spacing within a given zone. The resulting numerical procedure was substantially different from that employed in MIPPS-I; the only common elements in the two codes were the subroutines for physical property evaluation and interpolation.

Use of an explicit method simplified the code compared to the implicit solution method of MIPPS-I. While implicit methods are generally more stable than explicit methods and can therefore use larger time steps in the solution, the time-step in MIPPS-I was not limited by numerical stability but by the requirement that the interface advance no more than one cell per time step. Use of an explicit method was therefore expected to be advantageous in MIPPS-II.

MIPPS-II Results

As with MIPPS-I, an important mechanism predicted by MIPPS-II is the cyclical process of vaporization and condensation occurring in impulse drying, similar to a heat pipe mechanism. This means that the total volume of vapor in the sheet at any time is much smaller than it would be if all the evaporated water had remained in the vapor phase, an important fact which has been overlooked in some recent discussions of impulse drying. The continued phase-change heat transfer made possible by a broad two-phase zone greatly increases the heat transfer rate and fuels the displacement process.

Of particular interest are predictions for temperature propagation in a sheet, for part of the stimulus to develop MIPPS-II was recent temperature data in layered sheets showing some two-phase zone effects. Before discussing the predictions, a brief overview of some of the experimental data is in order.

In a study by Sprague [12], stacks of thin, wet sheets of bleached kraft paper were used, each sheet having a basis weight of 50 g/m². Extremely thin thermocouples were sandwiched between the sheets. During impulse drying with the MTS electrohydraulic press simulator, the temperature at each layer (including the felt-sheet interface) could be tracked in time. Tests showed that temperature propagation through a stack of thin sheets was essentially the same as temperature propagation through a single thicker sheet with the same cumulative basis weight, indicating that interface effects between the sheets were of minor concern.

Sample results are presented in Figures 3 and 4. Figure 3 shows the temperature at the felt-paper interface beneath a single 50 g/m² sheet. Three thermocouples at different locations on that interface were used, two of which gave nearly identical results; a significantly different third curve may have been due to a thermocouple problem or may be an indication of real nonuniformities. The upper two curves show traits found in several of the measurements: a steep S-shaped rise to a plateau above the ambient boiling temperature, followed by a rapid temperature rise which then levels off.

Measurements at three transverse locations are shown in Figure 4, where somewhat different trends can be seen. Here three 50 g/m² sheets have been stacked, and single thermocouples have been placed between the sheets. The upper curve from the thermocouple closest to the surface does not show an intermediate plateau as in Figure 3. The second curve, showing data from the interface between the middle and bottom sheets, does show an S-shaped rise followed by a nearly flat region. The thermocouple at the sheet-felt interface shows only a gradual temperature rise.

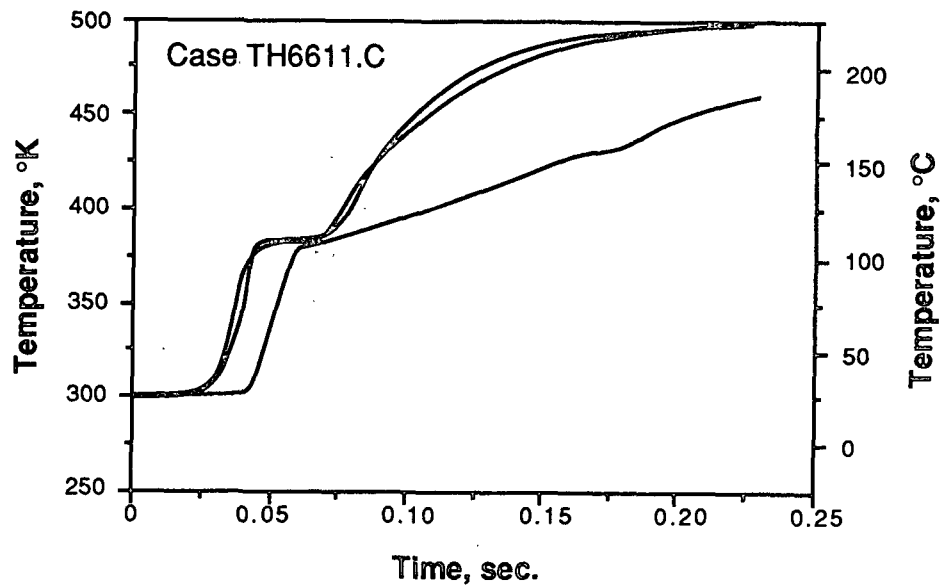


Figure 3. Temperature propagation at the backside of a single 50 g/m^2 sheet impulse dried with a head temperature of 530°K . Three thermocouples were placed at various locations on the paper-felt interface.

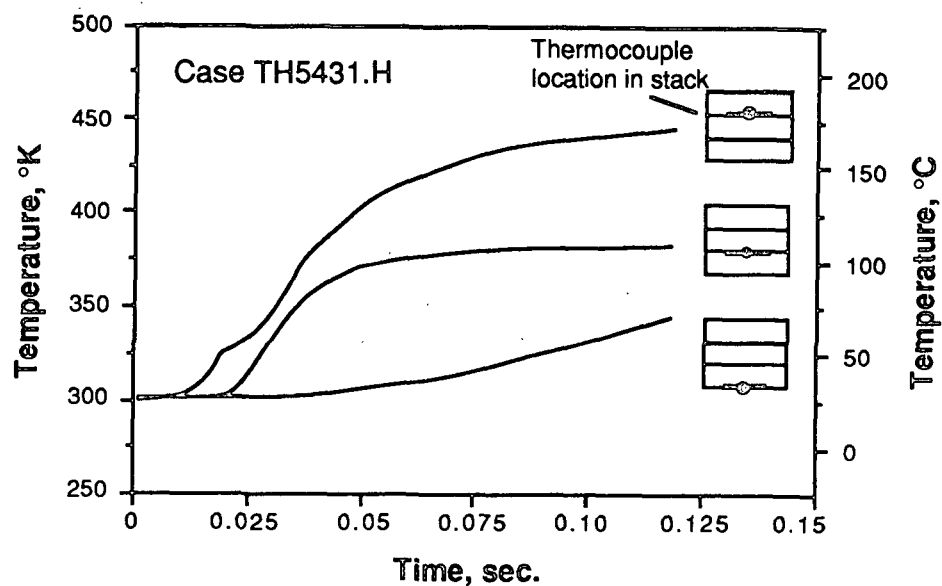


Figure 4. Temperature propagation at the inter-layer locations of a stack of three 50 g/m^2 sheets impulse dried with a head temperature of 260°C (530°K). Sheets lie on a felt.

The above results can be interpreted in terms of the vapor-liquid displacement concept. The existence of plateau regions somewhat above 100°C is strong evidence for a two-phase zone where the vapor and liquid are in equilibrium at an elevated pressure. The two-phase zone at any point may only be temporary, and as it is displaced or evaporated, a dry zone with higher temperatures follows. In some cases, the two-phase zone is very thin (or nonexistent), so a sharp steam-water interface may be a good description of the process. Regions of slow temperature rise, such as the bottom curve in Figure 4 or the initial period of the S-shaped regions during the first few milliseconds of impulse drying, show the effect of transient conduction heating through a saturated liquid zone. In short, the data are consistent with the proposed displacement mechanism of impulse drying, and provide new evidence that extended two-phase zones may be formed during impulse drying.

Predicted temperature histories from MIPPS-II at three sheet locations are shown in Figure 5. The predictions employed sheet properties and impulse drying conditions chosen for comparison with other MIPPS-I predictions, and may have no relation to those used by Sprague; the trends are the important thing for this comparison. Some of the same features seen in the experimental measurements are evident: an S-shaped transition from the initial temperature to a flat two-phase zone, which may be followed by a dry stage with a rising, concave-down curve. The close resemblance between the features seen in the data helps validate the treatment of the two-phase zone in MIPPS-II. The data do not always show a clear two-phase zone in the upper regions of the sheet, however, suggesting that some time may be required for a sharp interface to spread into a two-phase zone.

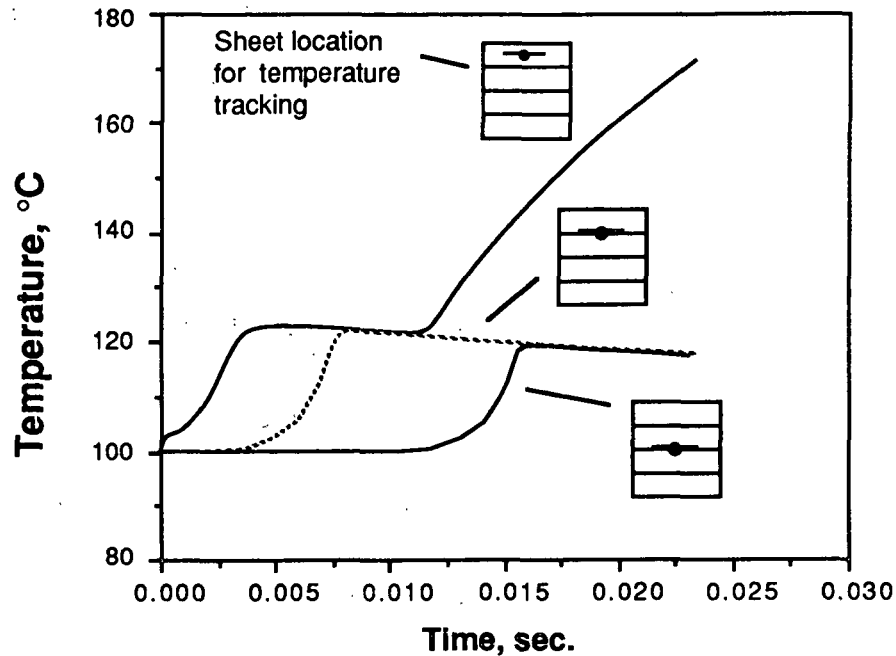


Figure 5. MIPPS-II predictions of local temperature histories in a 0.5 mm sheet with a permeability of $1.0 \times 10^{-14} \text{ m}^2$. Temperatures are tracked at locations corresponding to 1/8, 1/4, and 1/2 of the sheet thickness.

One interesting feature is the similarity between MIPPS-II predictions of interface motion and pressure development with similar predictions in MIPPS-I. Figures 6 and 7 compare MIPPS-II and MIPPS-I predictions of vapor pressure development and interface location, respectively, in a sheet of permeability $1.0 \times 10^{-14} \text{ m}^2$. Both predictions employed mild impulse drying conditions: the MIPPS-II predictions used a remaining water saturation of 0.1, and the MIPPS-I predictions used a capillary resupply rate of 0.1 kg/sm^2 . That the two predictions could be so similar is noteworthy (these were the first two sets of predictions to be compared, no trial-and-error was involved). This agreement suggests that the effect of residual water left in a two-phase zone is similar to the effect of water transported via insulated capillaries into a dry zone, and raises the possibility that either concept or both concepts have value.

Examination of boiling and condensation rates throughout the sheet during MIPPS-II predictions again show a continued process of boiling and evaporation. The rates of condensation are always close to the boiling rates near the hot surface. This phase change process gives high heat fluxes, beyond that of

conduction alone, which correlate with experimental results. A typical heat flux curve from MIPPS-II is given in Figure 8.

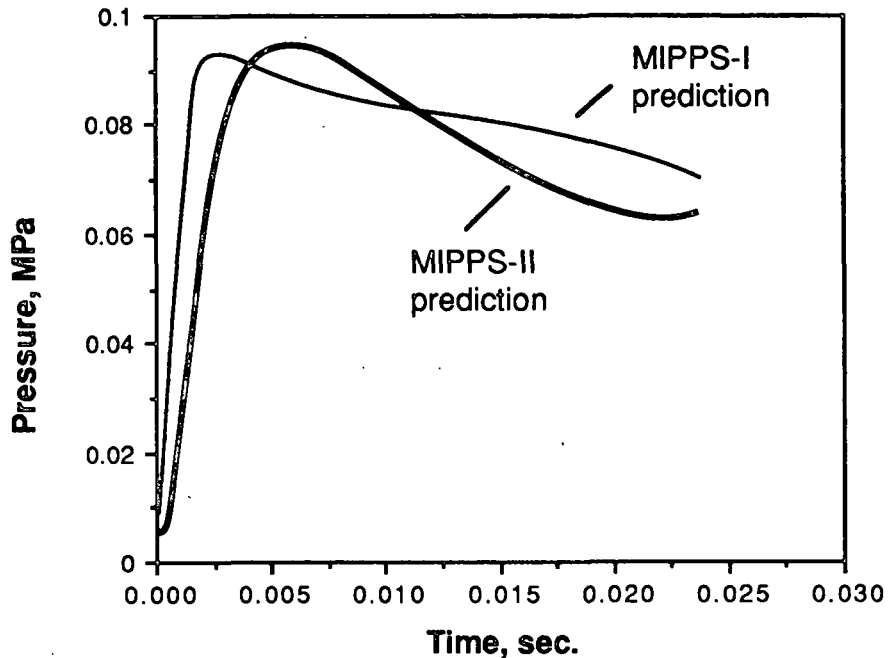


Figure 6. Comparison of predicted vapor pressure development in MIPPS-I and MIPPS-II. Sheet thickness was 0.5 mm, surface temperature was 330°C, and permeability was $1.0 \times 10^{-14} \text{ m}^2$. MIPPS-I used a wicking rate of 0.1 kg/sm^2 , and MIPPS-II used a remaining saturation value of 0.1.

MIPPS-II still has several serious limitations which will be addressed in the future. Compressibility of the porous medium is the most important feature which must be added. Treatment of capillary flow in the two-phase zone is also important. Furthermore, MIPPS-II has neglected the temperature gradients which may develop in the two-phase zone since regions of low saturation will have a higher equilibrium temperature than the more saturated zones.

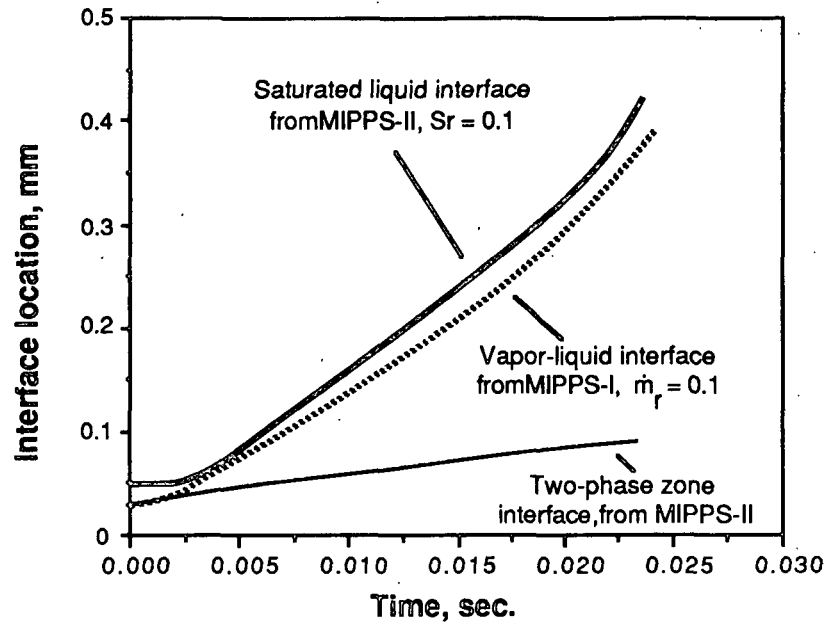


Figure 7. Comparison of interface motion predicted by MIPPS-I and MIPPS-II. Data are from the same computer runs used in Figure 6. MIPPS-II predictions include interface motion for the saturated liquid and the two-phase regions.

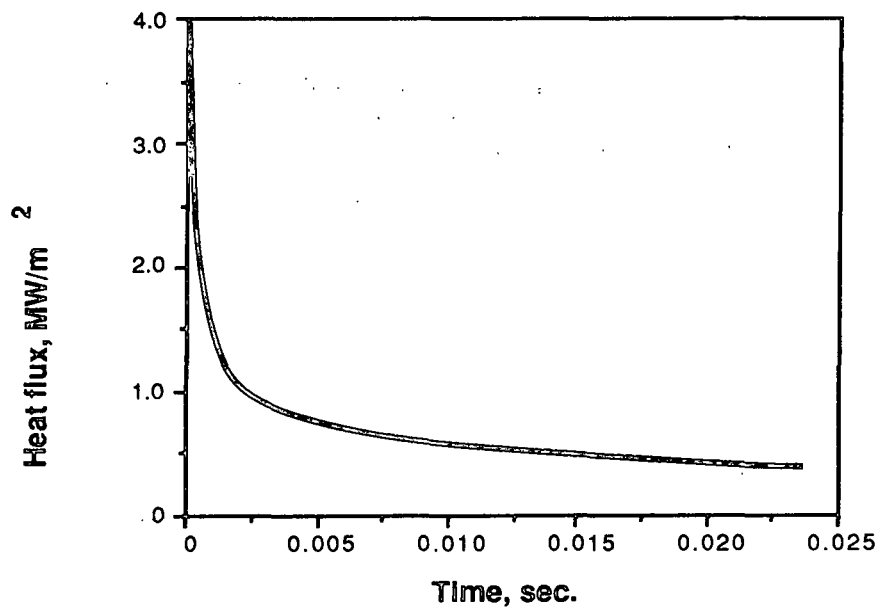


Figure 8. Heat flux predicted by MIPPS-II in a 0.5-mm sheet with permeability $1.0 \times 10^{-14} \text{ m}^2$ and S_r of 0.1.

The Anisotropic Permeability of Paper

The study of anisotropic permeability in paper [13] has been hindered by the demands on the MTS system as well, but a Carver press is now being modified to permit a continuation of this study. A separate student project was recently found to have relevance to the planar permeability of paper [14]; a collaborative effort is now underway to apply new numerical tools to extract anisotropic permeability data from the student's measurements. The student project involves the edgewise penetration of liquid into an evacuated disk of laminated paper, thus sealed on the upper and lower surfaces. A numerical method has been developed to relate the unevenness in liquid penetration to the MD-CD permeability ratio.

PLANS FOR NEXT PERIOD:

1. Conduct further experimental displacement work.
2. Continue refinement of MIPPS-II.
3. Complete modification of a Carver press to permit further measurements of anisotropic permeability in paper. Complete collaborative study of in-plane anisotropy in evacuated paper disks.

REFERENCES

1. Lindsay, J. D., Project 3480 Status Report to the Engineering Project Advisory Committee, The Institute of Paper Chemistry, Appleton, Wisconsin (Oct. 1988).
2. Lavery, H., Project 3470 Status Report to the Engineering Project Advisory Committee, The Institute of Paper Chemistry, Appleton, Wisconsin (Oct. 22, 1987).
3. Lavery, H. P., "New Mechanisms for Water Removal From Paper Through Impulse Drying," AIChE Summer Meeting, Minneapolis, Minnesota (Aug. 16-20, 1987). Also printed as IPC Technical Paper Series #251, The Institute of Paper Chemistry, Appleton, Wisconsin (July, 1987).
4. Macklem, E. A., and Pulkowski, J. H., "Impulse Drying- A Pressing/Flashing Drying Phenomena," 1988 Tappi Engineering Conference, Chicago, Illinois (Sept, 19-22, 1988).
5. Lindsay, J. D., Sprague, C. H., "MIPPS: A Numerical Moving Boundary Model for Impulse Drying," to appear in J. Pulp Paper Science (1989). Also presented at the CPPA Annual Meeting, Montreal (Jan. 26-29, 1988).
6. Lindsay, J. D., "The Physics of Impulse Drying: New Insights from Numerical Modeling," to be presented at the Ninth Fundamental Research Symposium, Cambridge, England (Sept. 16-22, 1989).
7. Rogers, J., "A Study of Rewetting in Impulse Drying Using Flash X-ray Radiography," M.Sc. Thesis, The Institute of Paper Chemistry, Appleton, Wisconsin (in progress, 1989).

8. Zavaglia, J., and Lindsay, J. D., "Flash X-ray Visualization of Multiphase Flow in Impulse Drying," to be presented at the 1989 Tappi Engineering Conference, Atlanta, Georgia (Sept. 1989).
9. Kloth, G., Sprague, C. H., and Hartman, T., "Water Movement in the Web of a Rolling Wet Press Nip Viewed with Flash X-ray Radiography," to be presented at the 1989 Tappi Engineering Conference, Atlanta, Georgia (Sept. 1989).
10. Dullien, F. A. L., Porous Media: Fluid Transport and Pore Structure, New York: Academic Press (1979).
11. Dullien, F. A. L., Chem. Eng. Journal; 10: 1 (1975).
12. Sprague, C. H., unpublished data, to be partially presented at Ninth Fundamental Research Symposium, Cambridge, England (Sept. 16-22, 1989).
13. J. D. Lindsay, "The Anisotropic Permeability of Paper: Theory, Measurements, and Analytical Tools," 1988 George Olmsted Award paper, American Paper Institute, available as IPC Technical Paper Series #289, The Institute of Paper Chemistry, Appleton, Wisconsin (1988).
14. Horstmann, D., M.Sc. Thesis, The Institute of Paper Chemistry, Appleton, Wisconsin (in progress, 1989).